

BIOCOMPATIBILITY STUDIES OF LAYER-BY-LAYER POLYELECTROLYTE COMPLEXES FOR BIOMEDICAL APPLICATIONS

A THESIS SUBMITTED TO THE GRADUATE SCHOOL OF APPLIED SCIENCES OF NEAR EAST UNIVERSITY

**By
MTHABISI TALENT GEORGE MOYO**

**In Partial Fulfilment of the Requirements for
the Degree of Master of Science
in
Biomedical Engineering**

NICOSIA, 2020

MTHABISI TALENT

GEORGE MOYO

**BIOCOMPATIBILITY STUDIES OF LAYER-BY-LAYER
POLYELECTROLYTE COMPLEXES FOR BIOMEDICAL
APPLICATIONS**

NEU

2020

BIOCOMPATIBILITY STUDIES OF LAYER-BY-LAYER POLYELECTROLYTE COMPLEXES FOR BIOMEDICAL APPLICATIONS

**A THESIS SUBMITTED TO THE GRADUATE
SCHOOL OF APPLIED SCIENCES
OF
NEAR EAST UNIVERSITY**

**By
MTHABISI TALENT GEORGE MOYO**

**In Partial Fulfilment of the Requirements for
the Degree of Master of Science
in
Biomedical Engineering**

NICOSIA, 2020

**Mthabisi Talent George MOYO: BIOCMPATIBILITY STUDIES OF
LAYER-BY-LAYER POLYELECTROLYTE COMPLEXES FOR
BIOMEDICAL APPLICATIONS**

**Approval of Director of Graduate School of
Applied Sciences**



Prof. Dr. Nadire ÇAVUŞ

**We certify this thesis is satisfactory for the award of the degree of Masters of Science
in
Biomedical Engineering**

Examining Committee in Charge:

Assoc. Prof. Dr. Terin Adalı



Supervisor, Department of Biomedical of
Engineering, Faculty of Engineering, NEU

Assist. Prof. Dr Ayşe A. Sarioğlu



Co-supervisor, Department of Medical
Microbiology, Faculty of Medicine, NEU

Prof. Dr. Tulin Bodamyali



Chairperson, Department of Health
Science, Faculty of Health Sciences, GAU

Assoc. Prof. Dr. Aylin Şendemir



Committee Member, Department of
Bioengineering, Faculty of Engineering, Ege
University

Assoc. Prof. Dr. Pınar Tulay



Committee Member, Department of Medical
Genetics, Faculty of Medicine, NEU

Assoc. Prof. Dr. Mahmut Ç. Ergören



Committee Member, Department of Medical
Biology, Faculty of Medicine, NEU

I hereby declare that all the information in this document has been obtained and presented in accordance with the academic rules and ethical conduct. I also declare that, as required by these rules and conduct, I have fully cited and referenced all materials and results that are not original to this work.

Name, Last name: MTHABISI TALENT GEORGE MOYO

Signature:

A handwritten signature in blue ink, consisting of stylized, overlapping loops and a long horizontal stroke at the bottom.

Date: 14/09/2020

ACKNOWLEDGEMENTS

Most importantly, my most sincere gratitude is to my thesis supervisor and course advisor Assoc. Prof. Dr. Terin Adali who devoted her time and effort to impart extremely valuable knowledge to me. In all times I found myself in need of assistance and a steer in the right direction, her office door was always open to me. I sincerely express my profound gratitude for her wisdom and kindness that has seen me through the accomplishment of this study. Without the passionate suggestions and input made by my jury members, I would not have been able to make the relevant improvements and rectifications to the study and for that I am eternally grateful.

I also thank Specialist Oğuz Han Edenbal, manager of the Biochemistry and Microbiology Laboratory at Near East University Hospital for his guidance through multiple experiments and Assoc. Prof. Dr. Ayşe Sarioğlu for her unwavering support. It is because of them that I did not have to blindly navigate particular sections of my research.

Finally, my family has been a continuous pillar of stability, encouragement and zeal, they have propelled me to where I am today, the appreciation I have for them and what they do for me is immeasurable. I should thank the numerous companions that I have counseled for help all through my studies. It is on their support, consolation and love that the foundation of this thesis is built.

**The future belongs to those who believe
in the beauty of their dreams...**

ABSTRACT

Tri-layer and bi-layer polyelectrolyte complexes films were synthesised from silk fibroin, chitosan and alginate using the solvent casting method to analyse their morphology, physicochemical properties, and biocompatibility properties together with the effects of their various interactions. The silk fibroin (SF), chitosan (CHI) and alginate (AL) products were characterized using differential calorimetry scanning (DSC), atomic force microscopy (AFM), and scanning electron microscopy (SEM) techniques. Thermograms from AFM demonstrated no bearing of the film thickness on number of layers but the dehydration properties of the outer most layer does. It was observed that PECs with SF as an outer layer showed to have the highest root mean square roughness R_{rms} (μm). As seen from the increasing crystallinity peaks and large differences in exothermic peaks, the results from the DSC analysis suggested that PECs with SF and CHI interactions and have the latter as an outer layer registers the best thermal stability. The SEM morphological images of all PECs with and without clopidogrel bisulphate (CLB) were studied, overall PECs infused with the anti-platelet agent highlighted assimilations of smooth and rough matrices of the drug with some having a heterogenous topography while others had rough clusters. In the contrary, SEM images of drug free PECs of the same PE composition were investigated and displayed very expanding porosity of composite films, which offers a more noteworthy cell adhesion factor. The cytotoxic effects of drug-loaded PECs were tested on the cell – line L-929 from rat fibroblast. The mesenchymal stem cells were harvested in standard culture conditions. The results of the cytotoxicity tests demonstrated that the drug-loaded blend of PE utilized in PEC film structure didn't support cell adhesion, cell development and differentiation for cell viability. Activity of antithrombosis was evaluated using prothrombin time (PT), standardized international ratio (INR), partially activated thromboplastin time (APTT), and total blood analysis using albumin and cholesterol. *In vitro* tests demonstrated that the clopidogrel bisulphate adjusted PECs affects platelet function, it showed that a surplus in the negative resting platelet charge differentiated with the primary reaction to clopidogrel bisulphate. Swelling kinetics of the different variations of PECs showed results that were indicative of pH-responsive swelling of all membranes in the definite pH run, clopidogrel bisulphate drug had an effect on the swelling kinetics.

Keywords: LbL PEC; solvent casting; chitosan; silk fibroin; alginate; clopidogrel bisulphate

ÖZET

Üç katmanlı ve iki katmanlı polielektrolit kompleks filmler, kimyasal, mekanik ve biyolojik özelliklerini çeşitli etkileşimlerinin etkileriyle birlikte analiz etmek için çözücü döküm yöntemi kullanılarak ipek fibroin, kitosan ve aljinattan sentezlendi. İpek fibroin (SF), kitosan (CHI) ve aljinat (AL) ürünleri, atomik kuvvet mikroskopisi (AFM), diferansiyel tarama kalorimetrisi (DSC) ve Taramalı elektron mikroskopisi (SEM) teknikleri kullanılarak karakterize edildi. AFM termogramları, tabaka sayısının film kalınlığı üzerinde hiçbir etkiye sahip olmadığını, ancak çoğu dış tabakanın dehidrasyon özelliklerinin olduğunu göstermiştir. Dış tabaka olarak SF'li PEC'lerin en yüksek ortalama kare kök pürüzleri R_{rms} (μm) olduğu görülmüştür. Artan kristallik tepelerinden ve ekzotermik tepelerde büyük farklılıklardan görüldüğü gibi, DSC analizinden elde edilen sonuçlar, SF ve CHI etkileşimli PEC'lerin ve dış katman olarak ikincisinin en iyi termal kararlılığı kaydettiğini düşündürmektedir. Klopidoğrel bisülfat (CLB) olan ve olmayan tüm PEC'lerin SEM morfolojik görüntüleri incelendi, anti-trombosit ajanı ile aşıl原因 genel PEC'ler, bazıları heterojen bir topografiye sahipken, diğerlerinin kaba kümeleri olan ilacın pürüzsüz ve kaba matrislerinin asimilasyonlarını vurguladı. Aksine, aynı PE bileşime sahip ilaçsız PEC'lerin SEM görüntüleri araştırılmış ve daha dikkate değer bir hücre yapışma faktörü sunan kompozit filmlerin çok genişleyen gözenekliliği sergilendi. İlaç yüklü PEC'lerin sitotoksik etkileri, sıçan fibroblastından hücre hattı L-929 üzerinde test edildi. Mezenkimal kök hücreler standart kültür koşullarında toplandı. Sitotoksikite testlerinin sonuçları, PEC film yapısında kullanılan ilaç yüklü PE karışımının hücre yapışmasını, hücre gelişimini ve hücre canlılığı için farklılaşmayı desteklemediğini göstermiştir. Antikoagülan aktivite, protrombin zamanı (PT), standartlaştırılmış uluslararası oran (INR), kısmen aktive edilmiş tromboplastin zamanı (APTT) ve albümin ve kolesterol kullanılarak toplam kan analizi kullanılarak değerlendirildi. *In vitro* testler, klopidoğrel bisülfat ayarlı PEC'lerin trombosit fonksiyonunu etkilediğini, negatif istirahat trombosit yükündeki bir fazlalığın klopidoğrel bisülfata birincil reaksiyonla farklılaştığını gösterdi. Farklı PEC varyasyonlarının şişme kinetikleri, sınırsız pH çalışmasındaki tüm membranların pH'a duyarlı şişmesini gösteren sonuçlarla, klopidoğrel bisülfat ilacının şişme kinetiği üzerinde bir etkisinin varlığını göstermiştir.

Anahtar Kelimeler: LbL PEC; çözücü dökümü; kitozan; ipek fibroin; aljinat; klopidoğrel bisülfat

TABLE OF CONTENTS

ACKNOWLEDGEMENTS	vi
ABSTRACT.....	iii
ÖZET	iv
TABLE OF CONTENTS	vi
LIST OF TABLES	viii
LIST OF FIGURES	ix
LIST OF ABBREVIATIONS	xii
CHAPTER 1.....	1
INTRODUCTION.....	1
1.1. Statement of Problem	5
1.2. Aim of the Study.....	5
1.3. Importance of the Thesis	5
1.4. General Objective.	6
1.5. Specific Objective.....	6
1.6. Thesis Outline.....	6
CHAPTER 2.....	8
LITERATURE REVIEW	8
2.1. Polyelectrolytes.....	8
2.2. Polyelectrolyte complexes (PEC)	8
2.3. Layer-by-Layer Polyelectrolyte Multilayer Systems	9
2.4. Clopidogrel Bisulphate release kinetics.	10
2.5. PECs for Wound Healing	11
CHAPTER 3.....	15
MATERIALS AND METHODS	15
3.1. Materials	15
3.2. Methods.....	15
3.2.1. Cleaning and Cutting.....	15
3.2.2. Degumming.....	15
3.2.3. Preparation of 0.1Mol Aqueous Solution.....	15
3.2.4. Dissolution.	16
3.2.5. Preparation of Electrolyte Solution.....	16
3.2.6. Dialysis.	16
3.2.7. Dissolution of Chitosan.....	17
3.2.8. Dissolution of Sodium Alginate.....	18

3.2.9.	Drug loading of LbL PECs.....	18
3.2.10.	Preparation of Layer-by-Layer PECs (Solvent casting).....	18
3.2.11.	Swelling Studies.....	19
3.2.12.	Preparation of Phosphate Buffer Solution.....	20
3.2.13.	Preparation of Acetic Buffer Solution.....	20
3.2.14.	Characterization of PEC's	20
3.2.15.	Cytotoxic evaluation of PEC's	20
3.2.16.	In-vitro hemocompatibility analysis of PEC's.....	21
3.2.17.	Prothrombin Time (PT).....	21
3.2.18.	Activated Partial Thromboplastin Time (APTT).....	21
3.2.19.	International Normalized Ratio (INR).....	22
3.2.20.	Total cholesterol	22
3.2.21.	Total albumin	22
3.2.22.	Measurement of LbL PEC thickness.....	23
CHAPTER 4.....	24
RESULTS AND DISCUSSION	24
4.1.	LbL PEC Synthesized.....	24
4.2.	Swelling studies	25
4.3.	Scanning electron microscopy (SEM)	27
4.4.	Differential scanning calorimetry (DSC).	39
4.5.	Atomic force microscopy (AFM)	43
4.6.	Cytotoxicity analysis	45
4.7.	PT, INR & APTT	49
4.8.	Total cholesterol test.....	50
4.9.	Albumin test	50
CONCLUSION	51
REFERENCES.....	52
APPENDICES.....	56
APPENDIX 1: ETHICAL APPROVAL DOCUMENT	56
APPENDIX II: SIMILARITY REPORT	58

LIST OF TABLES

Table 4.1: LbL PEC film composition.....	24
Table 4.2: DSC analysis of CLB loaded PECs where T_c °C - Exothermic Crystallization Peaks, T_M °C – Temperature Time Melting Point and T_D	39
Table 4.3: Properties of PECs measured by AFM.	45
Table 4.4: In-vitro coagulation test analysis results.....	49
Table 4.5: Total cholesterol test results.	50
Table 4.6: Albumin test results.	50

LIST OF FIGURES

Figure 2.1: Formation of polyelectrolyte complexes (Hubbe et al., 2015).....	9
Figure 2.2: Chemical structure of silk fibroin (Srisuwan & Baimark, 2013)	12
Figure 2.3: Chemical structure of chitosan (López-García et al., 2014).....	13
Figure 2.4: Chemical structure of sodium alginate (Srisuwan & Baimark, 2013).....	13
Figure 3.1: Purification steps of silk fibroin.	17
Figure 4.1: Swelling ratio of PEC-A to PEC-F in PBS pH7.4	25
Figure 4.2: Swelling ratio of PEC-1 to PEC-6 in PBS pH7.4.....	25
Figure 4.4: Swelling ratio of PEC-A to PEC-F in ABS pH 4.62.....	25
Figure 4.3: Swelling ratio of PEC-1 to PEC-6 in ABS pH 4.62.....	25
Figure 4.5: SEM micrographs showing morphological features of (a) PEC-A (b) PEC-B (c) PEC-C (d) PEC-D (e) PEC-E at 10µm.	27
Figure 4.6: SEM micrographs showing morphological features of (a) PEC-A (b) PEC-B (c) PEC-C (d) PEC-D (e) PEC-E at 20µm	28
Figure 4.7: SEM micrographs showing morphological features of (a) PEC-A (b) PEC-B (c) PEC-C (d) PEC-D (e) PEC-E at 50µm	29
Figure 4.8: SEM micrographs showing morphological features of (a) PEC-A (b) PEC-B (c) PEC-C (d) PEC-D (e) PEC-E at 100µm	30
Figure 4.9: SEM micrographs showing morphological features of (a) PEC-A (b) PEC-B (c) PEC-C (d) PEC-D (e) PEC-E at 500µm	31
Figure 4.10: SEM micrographs showing morphological features of (1) PEC-1 (2) PEC-2 (3) PEC-3 (4) PEC-4 (5) PEC-5 at 1mm	34

Figure 4.11: SEM micrographs showing morphological features of (1) PEC-1 (2) PEC-2 (3) PEC-3 (4) PEC-4 (5) PEC-5 at 20 μ m.....	35
Figure 4.12: SEM micrographs showing morphological features of (1) PEC-1 (2) PEC-2 (3) PEC-3 (4) PEC-4 (5) PEC-5 at 100 μ m.....	36
Figure 4.13: SEM micrographs showing morphological features of (1) PEC-1 (2) PEC-2 (3) PEC-3 (4) PEC-4 (5) PEC-5 at 200 μ m.....	37
Figure 4.14: DSC thermogram of PEC-A.....	40
Figure 4.15: DSC thermogram of PEC-B.....	40
Figure 4.16: DSC thermogram of PEC-C.....	41
Figure 4.17: DSC thermogram of PEC-D.....	41
Figure 4.18: DSC thermogram of PEC-E.....	42
Figure 4.19: AFM results of PEC-A.....	43
Figure 4.20: AFM results of PEC-B.....	43
Figure 4.21: AFM results of PEC-C.....	44
Figure 4.22: AFM results of PEC-D.....	44
Figure 4.23: AFM results of PEC-E.....	44
Figure 4.29: Concentration dependent in-vitro cytotoxic effect of PEC-E.....	49

LIST OF ABBREVIATIONS

ABS	Acetic Buffer Solution
AFM	Atomic Force Microscopy
AL	Alginate
APTT	Activated Partial Thromboplastin Time
CH	Chitosan
CLB	Clopidogrel bisulphate
DI	Deionized water
DSC	Differential Scanning Calorimetry
ECM	Extra Cellular Matrix
INR	International Normalized Ratio
LbL	Layer by Layer
PBS	Phosphate Buffer Solution
PE	Polyelectrolyte
PEM	Polyelectrolyte Multilayers
PEC	Polyelectrolyte Complex
PPC	Protein Polyelectrolyte Complexation
PT	Prothrombin Time
SEM	Scanning Electron Microscope
SF	Silk Fibroin
SR	Swelling Ratio
TE	Tissue Engineering
TGA	Thermogravimetric analysis
MSC	Mesenchymal Stem Cells
MI	Millilitre
WHO	World Health Organization

CHAPTER 1

INTRODUCTION

Ultra-significance of this indagation is in the elaboration and comparison of several test results using various combinations of Polyelectrolyte Complexes (PEC) (Silk fibroin, chitosan and alginate) cast Layer - by - Layer (LbL). There is an intrinsic focus on chemical, physical and biological properties of the PECs. This study will also focus on the analysis of their blood biocompatibility properties.

Over the last decade, researchers have taken a keen interest in the preparation and use of polyelectrolyte complexes from polymers that occur naturally to fabricate polyethene multi-layer biofilms, hydrogels, scaffolds, nano/micro-particles, and hydrocolloids (Ishihara et al., 2019). Instances of a few of these organically occurring polymers incorporate yet are not restricted to: negatively charged chitosan, silk fibroin and positively charged alginate. They have shown to possess impeccable biocompatibility (Bushkalova et al., 2019), excellent degradability (Nachimuthu et al., 2018), noncarcinogenicity (Ye et al., 2017), nonimmunogenicity (Ye et al., 2017) and biological activities such as surface properties including porosity, adhesion, differentiation, mortality, and proliferation (Muzzio et al., 2016). Blood biocompatibility studies of polyelectrolyte complexes are imperative because blood coagulation results are preliminary in concluding whether or not a material will be hemocompatible (Adali et al., 2019). The focus of LbL biofilms is imperative to important aspects of their application in Biomedical Science and Engineering, medicine and pharmacology disciplines. Hydrogen bonding, π π interactions, covalent bonding, hydrophobic interactions & charge transfer interaction are the driving forces behind their biocompatibility (Pahal et al., 2017). Cells choose to adhere to hard surfaces; mechanical stiffness is of great importance to PEC's because they have a vital role in the control of cellular to surface interaction. Moreover crosslinking is an important process on the mechanical properties of LbL PEC way of fine-tuning the biofilms (Gierszewska et al., 2018). These PEC's are precisely designed and controlled to suit various applications such as implant coatings, tissue scaffolding and wound healing (Ishihara et al., 2019). The greater part of the utilizations of PECs emerges from their properties (Muzzio et al., 2016). PEC films have various applications in biomedicine including wound healing, wound dressings, gene delivery, drug delivery, cell chemistry engineering, bio-adhesives, coatings to name a few (Pappa et al., 2017).

Layer-by-Layer (LbL) fabrication of attenuated polyelectrolyte biofilms continues to exhibit an effective and functional technique in the testing of types of biofilms and is undeniably fit to biomedical applications in light of the fact that the LbL fabrication is performed in vivo arrangement (Tu et al., 2019) . This technique exudes simplicity and versatility, taking this approach has an advantage of ionic attraction of the opposite ends of the films being the driving force of the experiments (Zhang et al., 2018). In 1992, Decher and co-scientists were the first to present this application alongside innovative biomedical applications alike to chemical and biosensors, assisted systems of drug delivery and electrochromatic apparatus, all based on the LbL assembly (S. Zhang et al., 2018). Biologically derived polymers such as alginate, chitosan, silk fibroin, collagen and hyaluronic acid over the past several years were intensively investigated for their drug delivery applications in biomedical science and in tissue engineering due to various their exquisite characteristics (Li et al., 2018).

The biomaterials to be utilized in the production of these PECs should be polycationic and polyanionic, since the polyelectrolytes (PE) are adsorbed by electrostatic interaction which will bring about the development of multilayer polyelectrolytes complexes (Ishihara et al., 2019). Polyelectrolyte multilayers (PEM) using this method will enable the layers to develop by elective adsorption of the polymers which will result in ultrathin functional membranes. (Landry et al., 2019). In this study, three important biocompatible polymers were used; Silk fibroin, Chitosan and Alginate.

Mesenchymal stem cells (MSCs) are multipotent undifferentiated cells that can separate into an assortment of cell types, including osteoblasts, adipocytes, chondrocytes, β -pancreatic islets cells myocytes and, possibly, neuronal cells (Han et al., 2019).

Fibroblasts are comprehensively scattered in various kinds of tissues, for instance, tendon, ligament and skin (LeBleu & Kalluri, 2018). Fibroblasts are by and large described as the cells that produce collagens and are seen as the fundamental wellspring of most extracellular matrix frameworks. They have a noteworthy impact in wound recovering (Dekoninck & Blanpain, 2019).

Cell lines are useful models for investigating cellular activity on different biomaterials as they give a great deal of unsurprising cells for deferred use (Han et al., 2019). Since most cell qualities are kept up in cell lines, they give reliable results (Muzzio et al., 2016). L929 cell line is commonly used as mechanical assembly in various standard testing. It is a cell line which is

celebrated in numerous assessment points of view, for instance, material biocompatibility testing, cytotoxicity testing and cell science (Behera et al., 2017).

The extracellular matrix (ECM) is a complex, heterogeneous arrangement of soluble and insoluble proteins, advancement factors, and polysaccharides that gives physical structure and a biochemical setting to the cell microenvironment (Vizovišek et al., 2019). ECM gives the mechanical framework to permit cell-cell interactions and upkeep (Krishtul et al., 2019).

It is important to mimic ECM because all cells that make up tissue are framed by ECM (Azizur Rahman, 2019). One strategy to make ECM-mimetic materials is the deliberate structure of protein-based planned ECM systems (Vizovišek et al., 2019). This separated structure strategy incorporates merging functionalities into a singular, estimated polymer course of action, realizing a multifunctional connect with self-sufficient tunability of the individual space limits (Xing et al., 2019). These ECMs routinely engage decoupled order over various material properties for head examinations of cell–cross section associations (Xing et al., 2019). Also, since the ECMs are routinely made through and through out of bioresorbable amino acids, these frameworks have immense clinical potential for a variety of regenerative drug applications (Scarritt et al., 2019).

Since thrombogenesis is a multifactorial strategy, examination of the thrombogenic activity of a biomaterial is and below very imperative in biomaterial manufacturing and research because researchers must make sure that when the material is administered to the human tissue, no haemorrhaging is formed (Adali & Uncu, 2013).

Silk fibroin, chitosan and sodium alginate are adaptable protein-polymers being incorporated into variety of associations to arrange physical, engineered fundamental and morphological features for specific biomedical applications (Tu et al., 2019). Anticoagulation activity is generally surveyed using prothrombin time (PT), activate partial thromboplastin time (APTT), international normalized ratio (INR) at different time extends (Adali & Uncu, 2013). The normal range for PT is 11 to 13.5 seconds (Adcock & Gosselin, 2017), the standard healthy range for APTT is 30 to 40 seconds but if the material has an antithrombogenic agent then the expected range is 120 to 140 seconds (Adcock & Gosselin, 2017) and the normal range for INR in healthy people is considered to be 1.1. A range of 2.0 to 3.0 is usually acceptable for patients taking antithrombogenic medication (Adcock & Gosselin, 2017).

Silk fibroin is a naturally occurring biomaterial complex originating from the bombyx mori silkworms, widely researched for its applications in biomedical research in tissue engineering

research due to its stellar biocompatibility, high mechanical properties and mild degradability (Adali & Uncu, 2013). Silk fibroin embodies an impeccable blend of solidarity, sturdiness just as a high limit of organic security that gives space upkeep to bone ingrowth while forestalling layer breakdown (Patil & Singh, 2019). It has been investigated that If treated, silk fibroin has very impressive capabilities. A research showed that sodium alginate converted the silk fibroin macromolecule and silk I into silk II. (Wang et al., 2016).

Chitosan is a cationic polysaccharide derived from co-polymers of N-acetylglucosamine associated by glycosidic bonds and glucosamine created by deficiently dissolved removal of acetyl groups in chitin (Ishihara et al., 2019). Chitosan is a biocompatible, biodegradable, cost-effective, environmentally friendly and energy sufficient material, studies have shown its ease in synthesis and characterization which makes it convenient for study purposes (Adali & Yilmaz, 2009). Chitosan advances brisk dermal recuperation alongside stimulating wound recovering by invigorating macrophages posing as a chemoattractant for neutrophils (Ishihara et al., 2019). Neutrophils are a type of white blood cells that invigorate immune system cells and expel dead cells in order to heal damaged tissues and resolve infection. Chitosan based biofilms and its subordinates have gained popularity in the biomedical field mainly for their immunological, wound recuperating, and antibacterial properties therefore are being utilised as a wound healing dressing (Tu et al., 2019).

Sodium Alginate is extracted from marine brown algae, a marine polysaccharide with high applicability in the development of hydrogel, thin film complexes, scaffolds and drug delivery systems (Yilmaz et al., 2019). Alginate is an elastic, irreversible hydrocolloid and a pH sensitive anionic polysaccharide, that becomes stable gel forms at low pH and acidic conditions but, swells and dissolves in alkaline pH. The major disadvantage of alginate-based delivery systems is rapid release of the loaded molecules. Therefore, it is modified either by crosslinking with multivalent cations or used in combination with different polymers, for example, chitosan (Gierszewska et al., 2018). 1-4 glycosidically connect guluronic acid and mannuronic acid which makes up the anionic copolymer (Hatami et al., 2017). The capacity of alginate as a protein conveyance gadget relies upon its atomic weight, and the overall level of the G and M units of alginate (Alshhab et al., 2019). Alginate has a similar make up structure to glycosaminoglycans (GAGs), a significant parts of extracellular matrix (ECM) in human tissue. Alginate is organic and easily biodegradable as it is an oceanic derivative (Hatami et al., 2017). It is generally utilized as a hydrogel after crosslinking with cationic divalent in various applications like tissue engineering of organs, injury recuperating and or drug

conveyance. Alginate dressings are preferred because they maintain moisture in the physiological microenvironment that advances quick epithelialization, wound recovery, and the development of granulation tissue (Bushkalova et al., 2019). Sodium alginate and chitosan biocomplex materials have different degrees of polycationic and polyanionic connections of polar charged polysaccharides (Coquery et al., 2019).

1.1.Statement of Problem

Ultrathin polyelectrolyte complexes have been designed as to the closest proximity of tuneable size and desirable properties to have many applications in the Tissue Engineering fields (S. Zhang et al., 2018). However, there is a constant demand of the study and production of PECs with stellar properties to be used in conjunction with the human body for various biomedical applications. Therefore natural polymers are preferable due to their relative biocompatibility and biodegradability (Ishihara et al., 2019). The layer-by-layer (LbL) deposition of materials by solvent casting has often been used to modify the surface of several materials. This technique has been used in application in the construction of nanostructured and easily tailorable three-dimensional self-standing structures (Kiziltay et at., 2019).

1.2.Aim of the Study

This research is aimed at preparing twelve layer-by - layer PECs with varying SF, AL & CHI compositions and improving their blood biocompatibility properties by modifying them with Clopidogrel bisulfate and comparing their morphology, physiochemics & biological properties to pure ones. The introduction of silk fibroin to an already studied chitosan-alginate complex was mandatory. An important goal was to embed the Clopidogrel bisulphate onto the LbL PEC films as a nonthrombogenic material without having a drastic effect on PT, IPTT an INR ranges of cholesterol, albumin and fibrinogen by using fresh human blood.

1.3.Importance of the Thesis

This study was effective study because there are few studies in the literature where different variations of SF, CHI and AL have been tried and compared. This study presents various mixtures prepared using some of the most suitable biomaterials in tissue engineering disciplines.

1.4.General Objective.

- Studying the intracomplexity effects, morphology, physiochemics and biological properties of polyelectrolyte complexes modified with silk fibroin, chitosan and alginate.

1.5.Specific Objective.

- Explanation of the significance of the study and its scope
- Description of silk fibroin, chitosan and alginate.
- Explanation of polyelectrolytes, polyelectrolyte complexes, layer-by-layer polyelectrolyte multi-systems and clopidogrel bisulphate.
- Steps in the purification of silk fibroin solution from its raw form through degumming, dissolution and membrane dialysis.
- Description in materials and methods used for chitosan and alginate synthesis.
- Solvent casting of layer-by-layer PECs and synthesis of drug loaded PECs
- Buffer solution preparation and triplicate swelling test.
- Characterization by- using SEM, DSC and TGA techniques and cytotoxicity evaluation.
- In-vitro biocompatibility tests including INR, PT and APTT.

1.6.Thesis Outline

The first chapter is inclusive of a generic introduction, study aim, significance of thesis, general and specific objectives of the thesis. In chapter 2, a literature review on polyelectrolytes, polyelectrolyte complexes, layer-by-layer polyelectrolyte multilayer systems, clopidogrel bisulphate and the wound healing application for PECs. The third chapter 3 details the materials and methods to be used in the experiments. Chapter 4

describes the results and discussion to follow. Finally, the thesis is concluded in the fifth chapter.

CHAPTER 2

LITERATURE REVIEW

2.1. Polyelectrolytes

Polyelectrolytes are macromolecular polymers with a dissociating electrolyte group in their repeat units. Polyelectrolytes contain positively or negatively charged ionic groups and can be divided into two groups polycations (+) and polyanions (-). Like ordinary electrolytes (acids, bases and salts), these can be dissolved in aqueous solution. After being put in any dissolvable ionizing chain forming a charged polymeric, polyelectrolytes separate into an exceptionally charged atomic polymeric form. The charge on the repeating units of that same PE is neutralized by opposite charged smaller counter ions which actually maintain the electrons neutral. If not, every polyelectrolyte solution contains a positive charged electrolyte. They may be ordered into different kinds relying upon the premise of their source, organization and sub-atomic engineering as well as may be characteristic polyelectrolytes, artificially altered polymers or manufactured (Meka et al., 2017).

2.2 Polyelectrolyte complexes (PEC)

Polyelectrolyte complexes (PECs) are 3-D macromolecules shaped by relationships of polar charged polyelectrolyte materials in arrangement. Polyelectrolytes (PEs) tend to shape edifices with at least one oppositely charged particles framing PECs. After crossing liquids of opposite charged PEs, a polyelectrolyte complex is created by effective prevailing electrostatic interactions between polycations and polyanions which cause the formation of a thick stage isolated from the dissolvable PE complexation that occurs fundamentally between opposite charging organisms. Composition and number of PECs acquired for the solidness, fixation, pH, quality of the ionic locales, blending proportion, ionic gathering nature, span and force, chain adaptability, sub-atomic weight, polymer structure, hydrophobicity, temperature, level of complexation, pH and ionic quality.

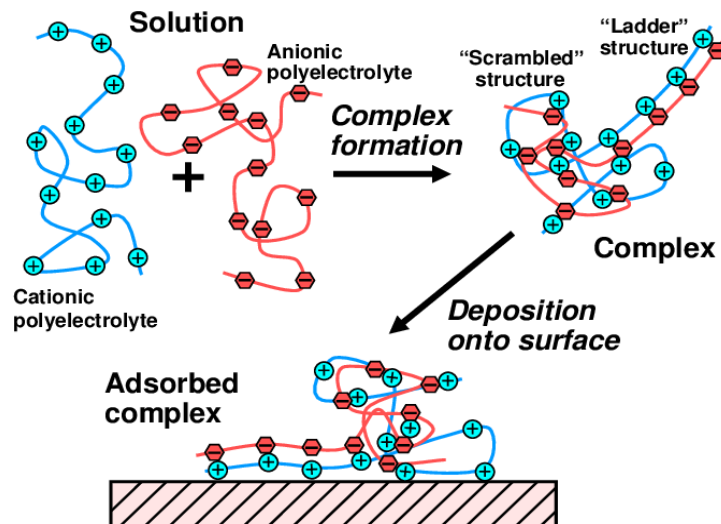


Figure 0.1: Formation of polyelectrolyte complexes (Hubbe et al., 2015)

PECs structure can significantly impact polymer dissolution rate, hydrodynamics, sedimentation, and permeability of the complex arrangement. New technology can also significantly alter the electrical conductivity, mechanical properties, and penetrability of frames. PECs can be seen as living systems ready to respond to environmental changes (Meka et al., 2017).

There are few types of PECS between common polymers, polyelectrolyte complexes between characteristic and manufactured polymers, polyelectrolyte complexes between engineered polymers, protein-polyelectrolyte complexes among polymers and opposite charged drugs and complex production between polyions and surfactants (Izumrudov et al., 2019).

2.3.Layer-by-Layer Polyelectrolyte Multilayer Systems

Polyelectrolyte multilayers (PEMs) may be viewed as a unique instance of PECs developed by utilizing a layer-by-layer (LbL) statement that includes consecutive testimony of sub-atomic thick polyelectrolyte layers with nanoscale command over the interior association, shape and size. Albeit numerous useful PEMs with novel synthetic and physical attributes have been created, the current reasonable utilizations of PEMs are constrained to ones requiring a couple of bilayers and are generally simple to plan. The feasibility of such designed materials can be acknowledged simply in the wake of defeating engineering and scientific drawbacks of understanding the transport and energy phenomena associated with the multilayer development and the components overseeing their arrangement, last structure and reaction to stimuli exerted externally (Sun et al., 2018).

The incorporation of multilayer polyelectrolytes in layer by layer (LbL) formation is an adaptable method for the creation of novel nanostructures and surface modifications. It comprises of few techniques including plunging assembly, casting assembly, spin assisted assembly, spray assisted assembly and alternative disposition. A plethora of PEC applications proposed include, but are not limited with the drug delivery systems, antibacterial coatings, polymeric materials, and bioelectronic gadgets (Xu et al., 2015).

2.4.Clopidogrel Bisulphate release kinetics.

Clopidogrel bisulphate (CLB) is an anticoagulant and specific antiplatelet agent that diminishes the danger of stroke in patients with intense coronary disorder, myocardial localized necrosis and other vascular illnesses. Clopidogrel bisulfate has become a drug of choice for patients who need an antiplatelet effect within hours prevention of heart attack. Clopidogrel 2-5 is a prodrug, which is metabolized into a metabolite that is pharmacologically active which inactive. This is used in ischemic accident control, myocardial infraction, stroke syndrome, epilepsy, panic disorder. This medication is an anti-platelet agent which inhibits platelets' ability to clump together as part of a blood clot. This drug is used either alone or with other drugs for stroke and heart attack prevention or treatment (usually caused by blood clots) in individuals at high risk.

Clopidogrel is a potent antiplatelet agent that minimizes the likelihood of thrombotic events in patients with atherothrombotic diseases frequently found to be higher than aspirin. Clopidogrel has been reported to be more effective than aspirin in decreasing the combined risk of ischemic stroke, myocardial infarction or vascular death (Kim et al., 2019). Clopidogrel bisulfate is soluble in acidic pH and degrades in base pH, so it seems a safe choice to generate gastro-retentive dosage (Chen et al., 2017).

Targeted lag time for the pulsatile formulation is 6 hours(h) followed by release of the drug burst to get the highest concentration in the morning. Average targeting time for tablet stomach retention was 7 to 8 hours(h) (Purohit et al., 2017).

Genetic polymorphisms involved in the absorption, metabolism, and the transporter P2Y12 of clopidogrel that interfere with its antiplatelet activity. Recent evidence indicates that epigenetic modification may also impair the response of clopidogrel's. In addition, the antiplatelet efficacy of clopidogrel may be affected by non-genetic factors such as ethnicity, disease complications and drug interactions. To increase platelet inhibition and reduce the

risk of cardiovascular events, the identification of factors leading to the variability in clopidogrel response is important (Purohit et al., 2017).

2.5.PECs for Wound Healing

Dermal wound healing is a perplexing procedure that incorporates four covering steps, specifically: inflammation, migration, multiplication and development stage. Generally, the recovery of epidermal tissue can happen immediately, contingent upon the size and profundity of the injury. Wound dressings should lock in moisture at the site of injury to support recuperating, bolster fibroblast development and guarantee solubilisation of development factors of potentially antimicrobial specialists. Therefore, low adherence to the surface of the injury, exuding assimilation and the capacity to exchange oxygen favours recovery. Chitosan meets preconditions such as hydrogel. (Blanpain et al., 2019).

The human body's rapid reaction to epidermal obstruction is haemostasis that happens at the exact place of the injury with the aim of minimalizing the discharge of blood and limiting haemorrhage. The first cells to arrive on site of the epidermal obstruction of injury are inflammatory cells and platelets. They do this by adhering to externally exposed collagen in the extracellular network. The platelets at that point discharge various proteins, for example on Willebrand factor (vWF), fibronectin, thrombospondin and sphingosine-1-phosphate in order to improve further incitement of platelets. The discharge of thickening variables animates fibrin framework to shape a steady coagulation which fills in as a temporary grid structure for cells relocating to the site of injury. (Jordan et al., 2019).

A favourable wound dressing ought to quicken tissue recovery to advance fast wound repair, should be nonantigenic, impervious to bacterial intrusion to forestall sepsis, and be nontoxic, demonstrate great adhering of complex to injury and simple to administer and expel. The wound dressing biomaterial must have great mechanical properties to maintain an integral structure and ideal moisture retention. (Daristotle et al., 2019).

For decades now PECs have been utilized as hemostats, tissue bio adhesives medication and cell conveyance transporters, injury dressings, and scaffolds for different tissue engineering applications. When bargained, wound healing might be guided by organic prompts, for example, Arg-Gly-Asp is a defined peptide for modifying cellular grip and relocation, which is subsequently accompanied by modified nanocarriers. Three distinct arrangements for prophylactic treatment were configured and analysed in vitro. Both plans

were based on carboxylated chitosan, and trimethylated. By combining two polar charged polymers of CMTMC and chondroitin sulphate in different polymer proportions, and representing b along these lines. *In vitro* studies showed no presence of poisonousness, capacity to advance expansion for more than 7 days, and advancement of human dermal fibroblasts treated with any of our definitions. These plans were shown to be ideal for simple topical application and can ultimately accelerate wound repair (Patrulea et al., 2019).

There are specific characteristics in wound dressings containing a silk fibroin complex that are found to be favourable such as cost effectiveness, moderate biodegradation, moderate toxicity levels, favourable immunogenicity, abundant availability, high limit with regards to water absorbance and great air porousness.

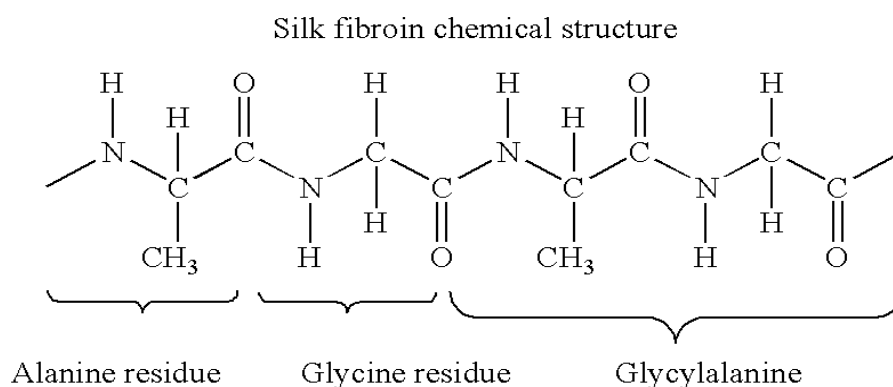


Figure 0.2: Chemical structure of silk fibroin (Srisuwan & Baimark, 2013)

Silk fibroin (SF) is a polymer with amazing mechanical properties such as flexibility, versatility (<35%), rigidity (0.525 GPa) and breaking extension (15%) (Kaplan et al., 2018). SF has high dissolvability in fluid, mainly those with salt arrangements and can be handily prepared into different structures, including films, nanofibers, hydrogels and wipes.

During wound healing chitosan interacts with numerous cells and cell processes. Chitosan has the potential to speed the recovery of wounds when administered as composite granules and powders, nano- and microparticles, wipes / sponges or composites with various biomaterials (Jordan et al, 2015).

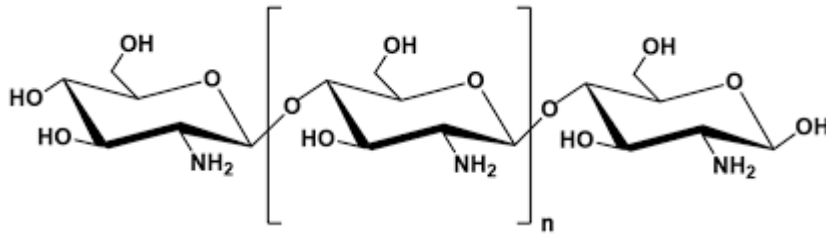


Figure 0.3: Chemical structure of chitosan (López-García et al., 2014)

In this way wounds are cleaned to remove debris therefore granulation tissue being framed permitting arrangement of fibrous tissue and re-epithelialization. On account that hypertrophic scars develop, mainly brought about by exorbitant collagen creation in the rebuilding stage, chitosan can diminish scar tissue, taking into account a decent re-epithelialization. Chitosan additionally influences the declaration of development factors inferred during the mending procedure.

A few investigations reported chitosan to advance granulation by actuating multiplication of dermal fibroblast and movement of polymorphonuclear neutrophils (Ikram et al., 2016). It was indicated that chitosan is engaged with all phases of injury mending. During the underlying recuperating stages, chitosan shows it's one of a kind hemostatic values and advances penetration and movement of neutrophils and macrophages.

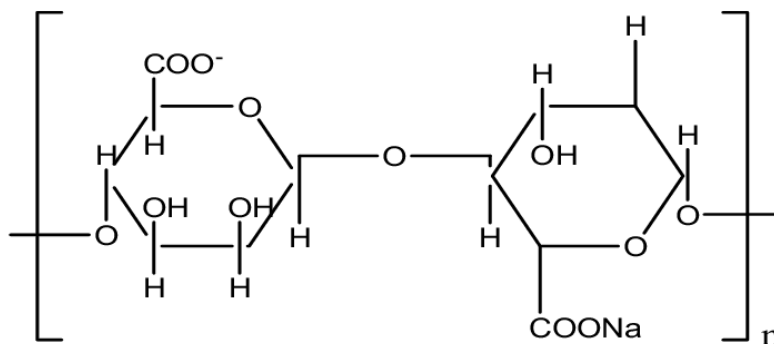


Figure 0.4: Chemical structure of sodium alginate (Srisuwan & Baimark, 2013)

Alginate wound dressings have magnificent biocompatibility. The crude material of the calcium alginate dressing is a kind of cellulose-like alginate corrosive separated from earthy colored ocean growth, namely seaweed, and this material is an ineffectively dissolvable

polysaccharide. Alginate dressings are a perfect filler, which is anything but difficult to crease and apply. Also, its capacity to absorb moisture is astounding.

CHAPTER 3

MATERIALS AND METHODS

3.1. Materials

Bombyx-mori cocoons, Sodium Carbonate (Na_2CO_3), Deionized Water (H_2O), Calcium Chloride (CaCl_2), Ethanol ($\text{C}_2\text{H}_6\text{O}$), Snake Skin Dialysis Tubing, Chitosan, Acetic Acid (CH_3COOH), Sodium Alginate, Sodium Tripolyphosphate (TPP), Techno Methacrylate (Di ethylene glycol di methacrylate), Clopidogrel Bisulphate and Methanol (CH_3OH).

3.2. Methods

3.2.1. Cleaning and Cutting

The cocoons obtained from the Bombyx-mori (silkworm) have to be cut into smaller pieces to enable degumming and cleaned to remove any unwanted dirt and impurities.

3.2.2. Degumming

Degumming is the process of removing the sericin, a gum-like protein that keeps the desired silk strands closely compacted together. This is done by using an analytical balance to measure the cut cocoons and place them in a conical flask, then preparing an aqueous solution to remove the sericin.

3.2.3. Preparation of 0.1Mol Aqueous Solution

In the analytical balance, 12g of Na_2CO_3 (Sodium Carbonate) powder was measured by using a graduated glass wear and placed in a beaker. A total of 200ml of deionized water was poured into a beaker with a magnetic stirrer. At 1rpm, the medium was electro-spun and allowed to spin till total dissolution in the beaker. After the Na_2CO_3 solution was ready the aqueous solution was poured into the conical beaker and placed on the magnetic stirrer at 70°C for three hours. Every hour for the recurring three hours, the aqueous solution of the similar quantities was prepared. Silk fibers were strained using a strainer and washed with pure water to further remove the sericin and they were placed in the flask. Aqueous solution was added in the flask and allowed to electro-spin. After the third wash, tweezers were used to separate the strands as finely as possible then left to dry. Double the ratio of both cocoons of solution for a higher volume of degummed silk fibers.

3.2.4. Dissolution.

Using a strong electrolyte solution, the air-dried silk fibers are placed in a beaker, and electro spun until total dissolution. Within solution a yellow pigment should be observed.

3.2.5. Preparation of Electrolyte Solution.

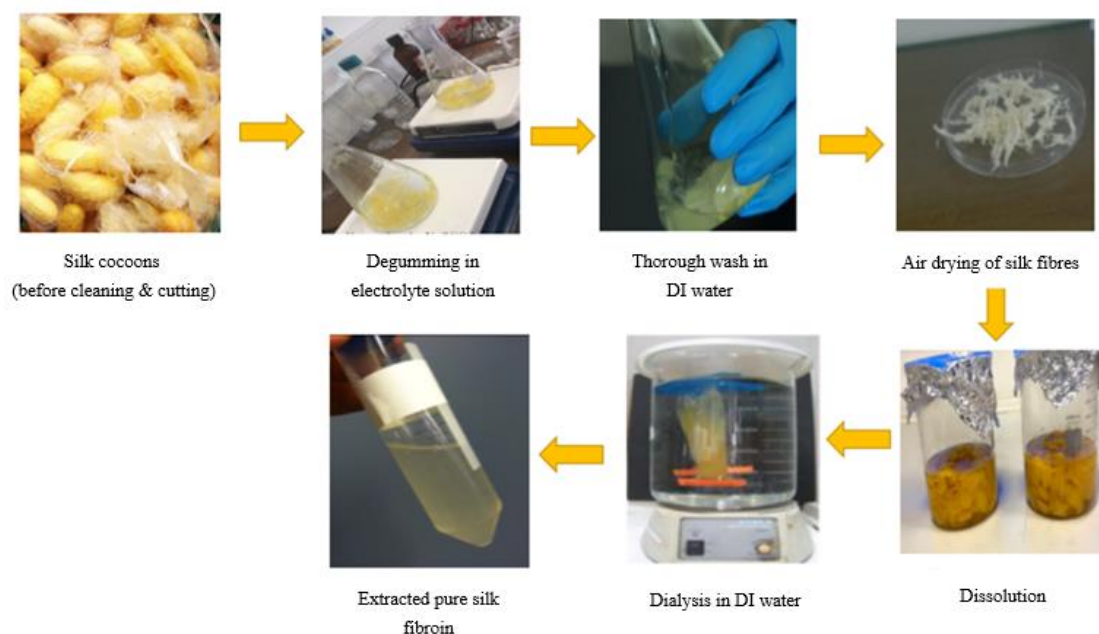
A total of 27.75g of calcium chloride (CaCl_2) was weighed and placed in a beaker and place it in a beaker. To start dissolving the CaCl_2 , 29.13ml of ethanol and 36ml of deionized water was poured into the beaker. Before spinning, the open rim of the beaker was covered with a parafilm and foil to avoid evaporation. Placed on a magnetic stirrer the solution was set to electro spin at 250rpm at 70°C. Before introducing the fibers to the beaker, the solution was heated up for 5 minutes. Bit by bit the fibers were placed in the strong electrolyte solution and allow to electro spin until they dissolved entirely.

3.2.6. Dialysis.

Dialysis, the process of removing salt from the liquid silk fibroin protein solution and the final steps for the purification of the solution. The concentrated SF solution was poured into a dialysis tube and then used larger beakers that totally immersed the dialysis tube and filled with deionized water. Depending on the desired concentration of silk fibroin, dialysis can be kept up over days and even weeks relying upon the capacity temperature, pH and grouping of silk arrangement. Thus, silk-based frameworks can be prepared utilizing aqueous solutions under mellow assembling conditions, for example, room temperature, impartial pH and without use of high shear power. The mentioned conditions were well used in several applications.

Using the quantity of SF at hand, the length of the dialysis membrane to be used was estimated (10cm). The snake membrane was cut using a sterilized scissors. One end of the hollow membrane was twisted and tightly tied with double twisted knots to prepare to close one end. Repeatedly, knots were tied to prevent outflow, ensuring that knots were secure. Using a sterile funnel to pour the dissolved silk into the membrane, reduce the space above the knot and secure the top end equivalent to sealing the bottom end of the membrane.

Distilled water was poured into a large beaker and placed on a magnetic stirrer with a rod set to spin at room temperature. The upper end of the membrane was tied the same way the bottom end was sealed. Onto a glass rod, one tied end of the membrane was latched on



using thread, making sure that the membrane does not come to contact with the beaker and doesn't fall in. It is vital to change the distilled water for every three hours for two consecutive days, leaving it in fresh deionized water over night. Upon dialysis, the pure Silk Fibroin is obtained using a sterile syringe and suctioned into a Falcon Conical Centrifuge tube.

Figure 0.1: Purification steps of silk fibroin.

3.2.7. Dissolution of Chitosan.

A total of 3g of chitosan was measured and placed in a beaker. Further, 100ml of 0.1M acetic acid was added into the beaker and placed on the magnetic stirrer with a magnetic stirring rod. The solution was allowed to spin until the solution totally dissolved.

A standardized grammage of its raw form has been used for different percentages of concentration, depending on the percentage required for the chitosan. To obtain 1% chitosan a gram of granulated chitosan that is put and spun slowly to dissolve in 100ml of acetic acid. To obtain 2% chitosan, in 100ml acetic acid, add and let to spin 2g of chitosan

until total dissolution. The recurring percentages use the same ratio. chitosan is dissolved in acetic acid as it is insoluble in water.

3.2.8. Dissolution of Sodium Alginate.

In a weighing balance, 2g of sodium alginate powder was weighed and placed in a beaker. In the same beaker 100ml of distilled water was poured in. A magnetic stirring rod was also placed into the beaker on a magnetic stirrer at 100rpm until total dissolution was observed.

Depending on the percentage required for the alginate, a standard grammage of alginate is used for different percentages of concentration in distilled water (100ml). To obtain alginate solution with a concentration of 1%, one gram of alginic acid is spun in 100ml of distilled water until total dissolution. To obtain Alginate solution with a concentration of 2%, two grams of alginic acid are spun in 100ml of distilled water until total dissolution. The recurring percentages will follow suit in ratio.

3.2.9. Drug loading of LbL PECs

Sixty milligrams of clopidogrel bisulphate drug were measured and placed in a small beaker. The measured drug was dissolved in 10ml of acetic buffer solution (ABS) with pH. 1.2 and placed on a magnetic stirrer until the drug was totally dissolved.

For every 1ml of polyelectrolyte solution to be used in the PEC film layering, mixture with 3mg of the drug was prepared.

3.2.10. Preparation of Layer-by-Layer PECs (Solvent casting).

Syringes that were used in the experiments were disinfected by washing with distilled water and ethanol before use. Inserting the required amount, the required material (silk fibroin, chitosan or alginate) was drawn into the syringe. The polyelectrolyte complex (PEC) was discharged onto a sterile glass petri dish and spread evenly across the surface by moving it in dipped circular motions and left to dry overnight. In this study, the best bio-films were formed by leaving the liquid to dry overnight, placing it on a heated magnetic stirrer made the bio-films brittle and susceptible to cracking. If need be, using a pipette or micro pipette,

a cross-linker may be used to strengthen the film morphology. The required materials were added layer by layer, and each layer was allowed to dry at each step.

To extract the biofilms from the petri dish, methanol was poured to immerse the thin film and let to rest for 30-45 minutes. After the suggested time, sterilized tweezers were used to check if the bio-film was removable. If the bio-film peeled off well, then we carefully peeled it off avoiding cracking and extracted. If not, we let it stay in methanol for longer.

3.2.11. Swelling Studies.

Several LbL PEC with varying ratios of chitosan, silk fibroin and alginate were developed respectfully to protocol and submerged into two solutions with the aim of studying their swelling properties, namely weight and swelling ratio over time. The solvents used were PBS at pH 7.4 and ABS at pH 4.62. PBS mimics the ECM of the human bone marrow, venous blood, arterial blood and heart capillaries. Acetic buffer solution (ABS) mimics the internal cellular environment.

Swelling test procedure includes measuring and cutting two 2cm×2cm PEC, one to be tested in a PBS and the other for ABS. Ten sterile glass bottles were labeled, two for each sample. Eight ml of each solution was measured and poured into the appropriately labeled glass bottle. A table with time intervals that range from 5minutes to 150minutes was plotted to record the weight as time progressed. Before immersing the samples in the solution, their dry weights were weighed on a weighing balance and was recorded accordingly. In each glass bottle respectively, placed each PEC in one buffer solution then immediately after placing another biofilm in the other solution, took time and allowed to swell for the periodic time. After each interval, the wet film was blotted with filter paper to remove excess solution, placed in the weighing balance and recorded. The swelling ratios were calculated by using the following equation:

$$Swelling\ Ratio\ (\%) = \left(\frac{weight_s - weight_{dry}}{weight_{dry}} \right) \times 100\% \quad (3.1)$$

3.2.12. Preparation of Phosphate Buffer Solution.

A total of 1.4196g of Sodium Hydrogen Phosphate (Na_2HPO_4) was measured and placed in a beaker with 100ml of deionized water. A magnetic stirring rod was placed in the beaker allowing the solution to spin on the magnetic stirrer at 100rpm and heat at 60°C until total dissolution was observed. The assumed pH with these measurements was 9.356. Hydrochloric acid is used to reduce the pH.

3.2.13. Preparation of Acetic Buffer Solution.

In a large beaker, 800 mL of distilled water and 7.719 g of anhydrous sodium acetate were added to the beaker. Then, 0.353 g of acetic acid was added to the solution and HCl (or NaOH) was used to adjust to the desired pH. Distilled water was added until volume was 1L.

3.2.14. Characterization of PEC's

Samples were characterized by scanning electron microscope (SEM) for the perception of the surface morphology utilizing Quanta 400F field Au-Pd covering. Atomic force microscopy (AFM) using the Veeco MultiMode V instrument was used to analyze the geology of the surface and topography, and differential calorimetry scanning (DSC) was carried out using Perkin Elmer, Pyris 6 DSC method.

3.2.15. Cytotoxic evaluation of PEC's

The ultra violet (UV) light for sterilization purpose irradiated both sides of the PECs. The Minimum Essential Medium Eagle (EMEM, M2279, Sigma Aldrich, Germany without serum) with a concentration of 0.2 g / mL was collected at 37 ± 0.1 ° C, 24 h in growth culture. ISO 10993-12:1998 was used for process extraction. The dilution of material extraction has been carried out at 50 %, 25 %, 12.5 % and 100 % extract material. Ten percent Fetal Bovine Serum (FBS, A0500-3010, Cegrogen Biotech, Germany), containing 1 % Sodium Piruvate (L0473, Merck, Germany), 0.1 % Penisilin-Streptomisin (A2213, Biochrom, Germany) was used.

The cell – line L-929 from rat fibroblast was selected according to the ISO 10993-5:2009 *In vitro* Cytotoxicity Tests Standards. The selected cells passage number was in between 8 -10. Approximately 1×10^5 cells / mL of each well were seeded in 96 well plates with 100

ul volume per well. After 24 hours of incubation at 37 ° C, 5% CO₂ and 95% moisture, four separate concentrations of cells were cultivated (100%, 50%, 25% and 12.5%). PEC sample cytotoxicity analysis was conducted using the MTT (3-(4, 5-Dimethylthiazol-2-yl)-2,5-Diphenyltetrazolium Bromide) assay. Control group without PEC sample was standard cell culture medium. After 24 h culture medium was extracted from wells and 10 per cent MTT (5 mg / ml) was incubated at 4 h, including EMEM. After incubation period, DMSO (802912, Merck Germany) was added to the system after removal of MTT containing medium. With the help of DMSO, formazan crystals were dissolved. The microplate reader (Synergy HTX, BioTeck, USA) was used for absorbance measurement at 570-690 nm wave lengths.

3.2.16. In-vitro hemocompatibility analysis of PEC's.

Parameters of coagulation were examined, three LbL PEC samples PEC-1, PEC- and PEC-E were submerged into fresh blood that was donated by human benefactors issued by Near East University Hospital, Northern Cyprus. STA Compact was used for the measurement of coagulation parameters. Using 3.2% trisodium citrate in siliconized vacutainer tubes, the blood samples were thinned and anticoagulated for a proper procedure. Caution was taken to note adequate filling of the collection tubes. Ensuring that only specimens that had a 9:1 ratio of venous blood to anticoagulant citrate were used was important. Thirty minutes after sampling, the mixture was centrifuged inside at 850rpm for 10 minutes. APTT, INR, and PT are measured automatically by generic reagents Stago STA-Neoplastine CI plus and Cephascreen. Test results in INR, and seconds.

3.2.17. Prothrombin Time (PT)

Time for prothrombin was measured using sample plasma. The venous blood was inserted into a test tube filled with citrate to separate the plasma from the other blood cells. This was achieved by adding the calcium that serves as an antiplatelet and centrifuged from the venous blood cells to remove the plasma. The time it takes for the sample to coagulate was determined after adding factor II (Tissue factor).

3.2.18. Activated Partial Thromboplastin Time (APTT)

New samples of human blood were collected in citrate-coated tubes to imbroglia the calcium and to avoid the coagulation. Adding calcium to the tube would have an inverse

effect on the oxalate's anticoagulant effects, and an activator was mixed into the plasma test. Information from *in vitro* investigations was assessed utilizing two-route investigation of change (ANOVA) to evaluate contrasts in hemolytic exercises between the altered examples and untreated silk fibroin (SF).

3.2.19. International Normalized Ratio (INR)

The International Standardized Ratio (INR) uses the International Sensitivity Index (ISI) to equate all thromboplastins to the reference thromboplastin performed to normalize prothrombin time (PT). The INR depends on the proportion of prothrombin time of the patient and the usual mean prothrombin time. Prothrombin duration is a blood test that tests how long it takes for patients to get oral anticoagulant medication to filter the blood. The INR uses the ISI to equate all thromboplastins with the reference thromboplastin by the corresponding condition in which ISI is the universal sensitivity index of the checked thromboplastin.

$$INR = \left(\frac{\text{patient PT}}{\text{mean normal PT}} \right)^{ISI} \quad (3.2)$$

3.2.20. Total cholesterol

Blood samples were collected by standard venipuncture techniques into plastic tubes was used. Complete clot formation was ensured before centrifugation and serum sample was used in the study. This test is based upon an enzyme-assisted response to detect free esters of cholesterol and cholesterol. Cholesterol esterase transforms esterified cholesterol into cholesterol which is then added to produce ketone, cholest-4-en-3-one product and hydrogen peroxide by cholesterol oxidase. The sensitive stable fluorescence probe detects the hydrogen peroxide.

3.2.21. Total albumin

Typically, determining serum albumin involves salt fractionation, utilizing high speed centrifugation, electrophoretic or dye restricting strategy. Dye restricting systems are simply the least difficult to perform, and loan to high volume testing and computerization.

Test tubes were labelled and using a pipette 1.0 ml of reagent into each cylinder was placed. 0.01 (10ul) of test sample was placed to particular cylinders and mixed. All cylinders were incubated at room temperature for one minute. Spectrophotometer was zero with the clear at 630 nm. Several absorbance values were recorded.

3.2.22. Measurement of LbL PEC thickness

Knowing biofilm thickness a significant parameter that scientists and researchers should know as it identifies to have a relation with the development of the biofilm and the degree to which biofilms interact with human designed gadgets. The rate at which supplements and antimicrobics enter biofilms is identified with thickness, just like the rate to which they react to antimicrobics like disinfectants and anti-microbials. How much biofilms meddle with the fouling of channels and liquid conveyance frameworks and meddle with the capacity of gadgets like warmth exchangers is likewise due, to some extent, to the profundity of the bio-film. Thickness was estimated utilizing the atomic force microscope.

CHAPTER 4

RESULTS AND DISCUSSION

4.1.LbL PEC Synthesized

Table 4.1: LbL PEC film composition

PEC LbL films	Composition
PEC-A	2.5ml 2% CHI + 2.5ml 2% SF + 2.5ml 2% CHI + 22.5mg Clopidogrel bisulfate
PEC-B	2.5ml 2% SF + 2.5ml 2% CHI + 15mg Clopidogrel bisulfate
PEC-C	2.5ml 2%SF + 2.5ml 2%CHI + 2.5ml 2%SF + 22.5mg Clopidogrel bisulfate
PEC-D	2.5ml.2% AL+ 2.5ml 2%SF + 2.5ml 2%CHI + 22.5mg Clopidogrel bisulfate
PEC-E	2.5ml 2% AL + 2.5ml2%SF + 2.5ml2% AL + 22.5mg Clopidogrel bisulfate
PEC-F	2.5ml 2%SF + 2.5ml 2%AL + 15mg Clopidogrel bisulfate
PEC-1	2.5ml 2% CHI + 2.5ml 2% SF + 2.5ml 2% CHI
PEC-2	2.5ml 2% SF + 2.5ml 2% CHI
PEC-3	2.5ml 2%SF + 2.5ml 2%CHI + 2.5ml 2%SF
PEC-4	2.5ml 2% AL + 2.5ml.2%SF + 2.5ml 2%CHI
PEC-5	2.5ml 2% AL + 2.5ml2%SF + 2.5ml2% AL
PEC-6	2.5ml 2%SF + 2.5ml 2%AL

4.2. Swelling studies

Swelling ratios of PECs in PBS pH 7.4 and ABS pH 4.62 were:

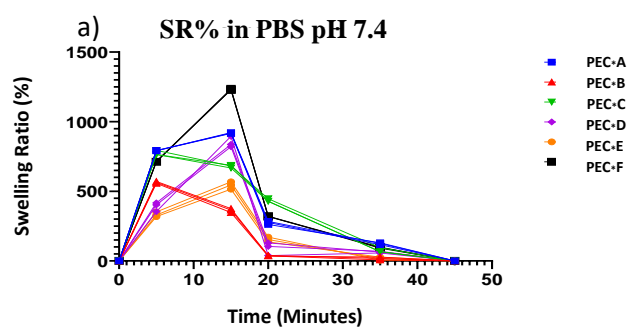


Figure 0.1: Swelling ratio of PEC-A to PEC-F in PBS pH7.4

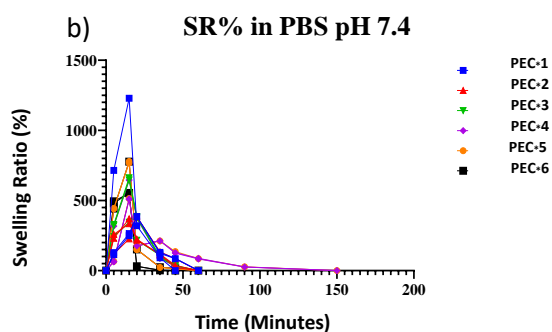


Figure 0.2: Swelling ratio of PEC-1 to PEC-6 in PBS pH7.4

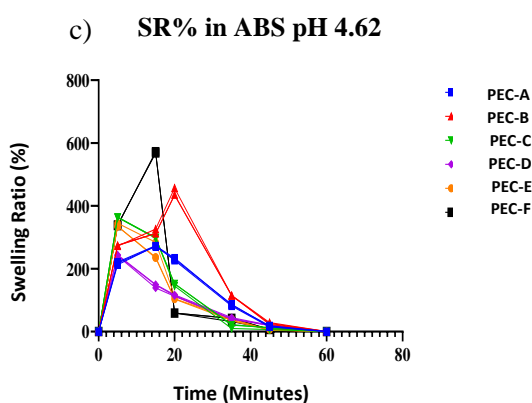


Figure 0.3: Swelling ratio of PEC-A to PEC-F in ABS pH 4.62

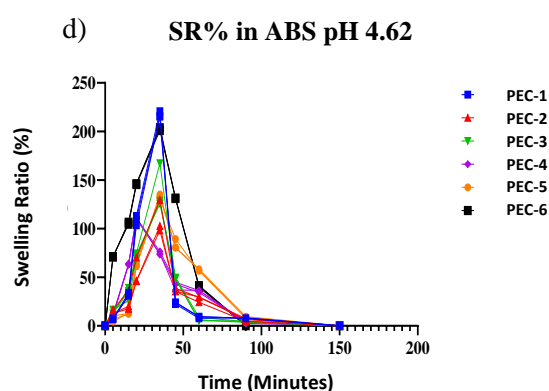


Figure 0.4: Swelling ratio of PEC-1 to PEC-6 in ABS pH 4.62

Swelling kinetics of the developed PEC's were studied in two solution buffers of different constant ionic strengths. Figure. 4.1 to Figure. 4.4 present the dynamic swelling data for polyelectrolyte membranes loaded with drug and without drug. As can be observed in Figure. 4.2, drug free PEC's swelled and disintegrated quickly in PBS. The results of drug loaded membranes showed that they had an elevated resistance to dissolution, however was stable

at pH 4.62 but were the quickest to dissolve in PBS ant pH 7.4. but had the least swelling ratio over time in ABS pH 4.62. The results are indicative of pH-responsive swelling

of all membranes. CHI/SF/CHI and SF/AL films showed a significant swelling peak in pH concentrations. Evidently the clopidogrel bisulphate drug had an effect on the swelling kinetics because the PECs disintegrated fully within 60 minutes. The AL / SF / CHI complex displays the longest equilibrium with and without medications, at both high and low pH. Throughout the definite pH phase, all samples experienced substantial volume and additional mass shift.

4.3. Scanning electron microscopy (SEM)

SEM has observed morphological features of LbL PECs embedded with clopidogrel and solely without drug infusion. The figures below show the SEM micrographs.

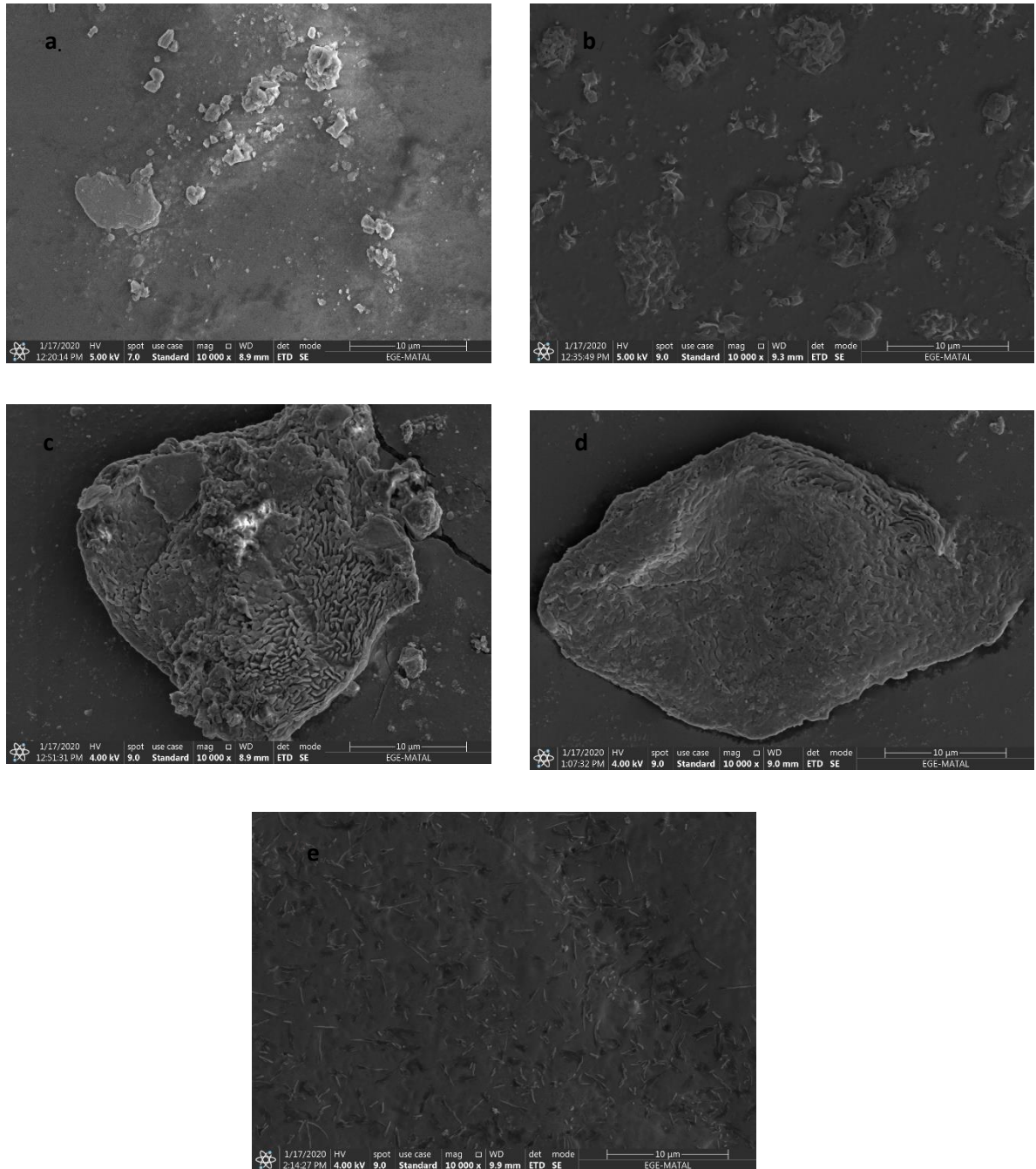


Figure 0.5: Morphological features (a) PEC A (b) PEC B (c) PEC C (d) PEC D (e) PEC E at 10μm.

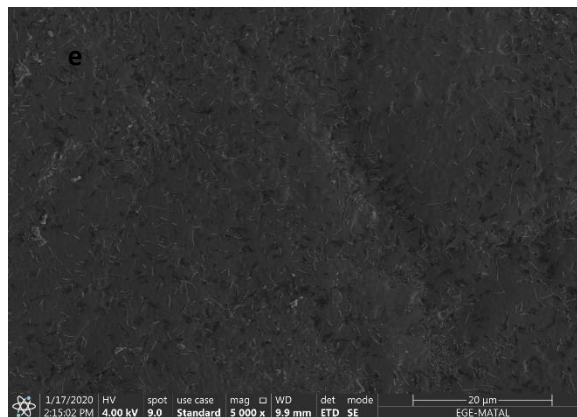
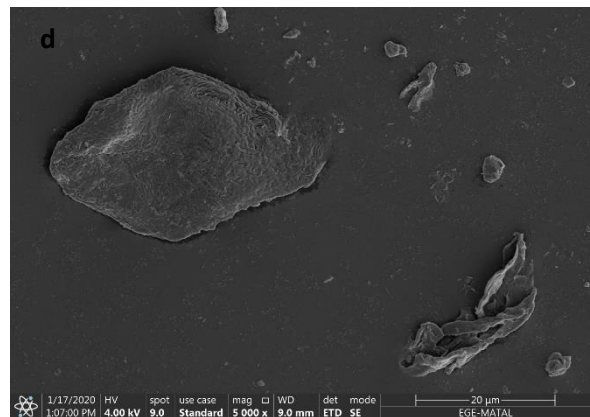
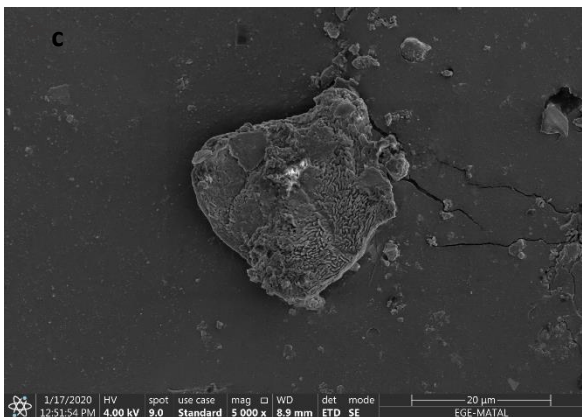
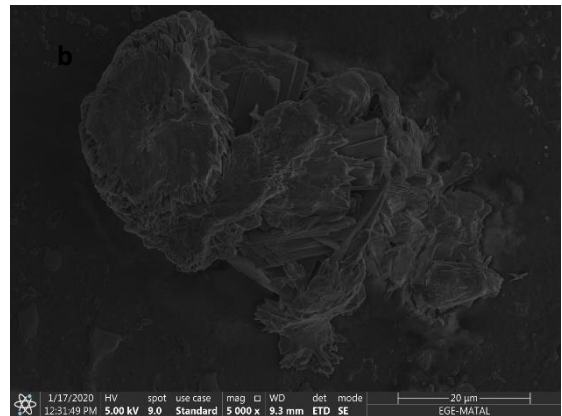
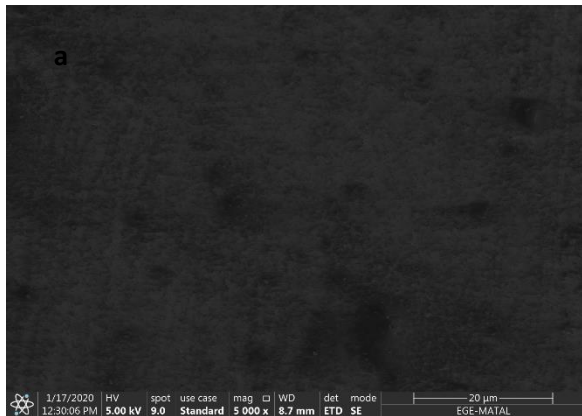


Figure 0.6: morphological features (a) PEC A (b) PEC B (c) PEC C (d) PEC D (e) PEC E at 20 μ m

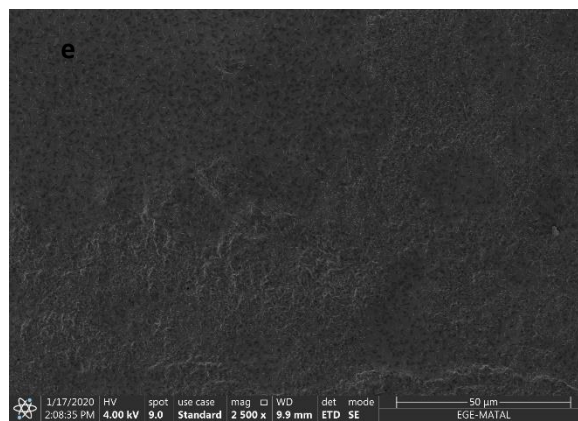
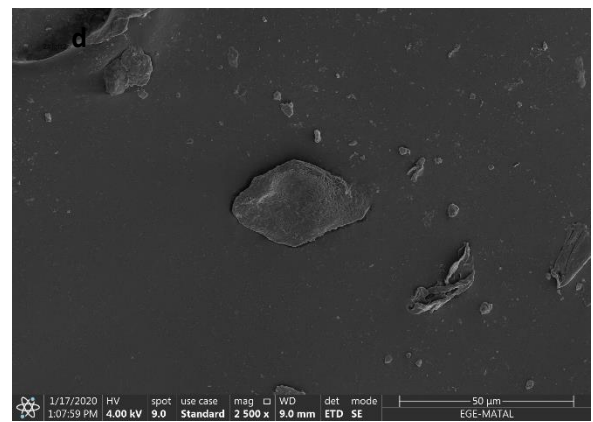
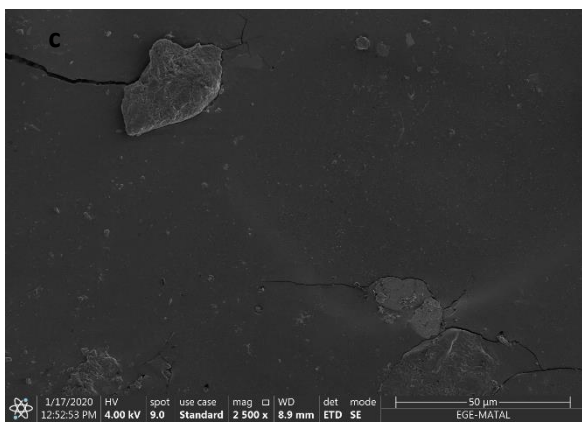
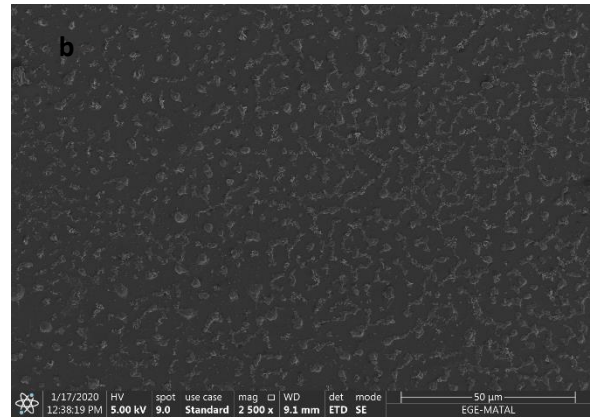
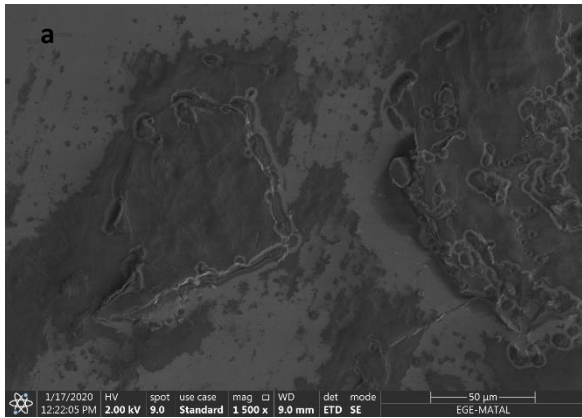


Figure 0.7: morphological features (a) PEC A (b) PEC B (c) PEC C (d) PEC D (e) PEC E at 50μm

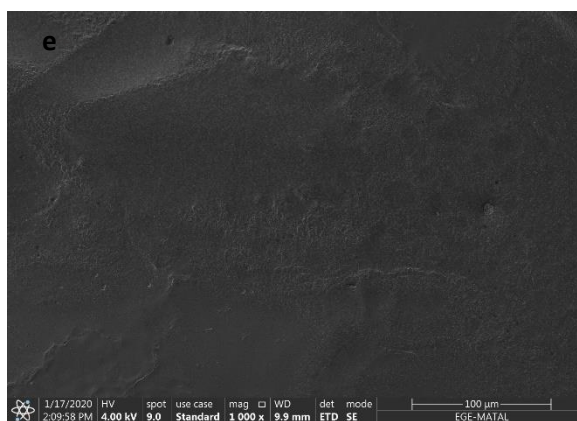
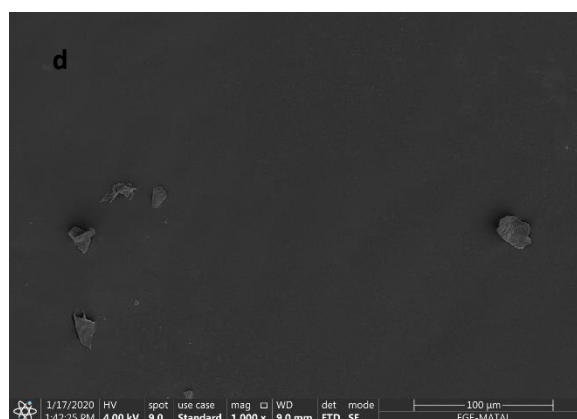
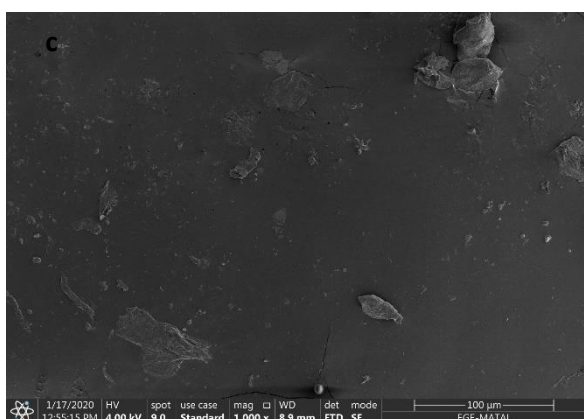
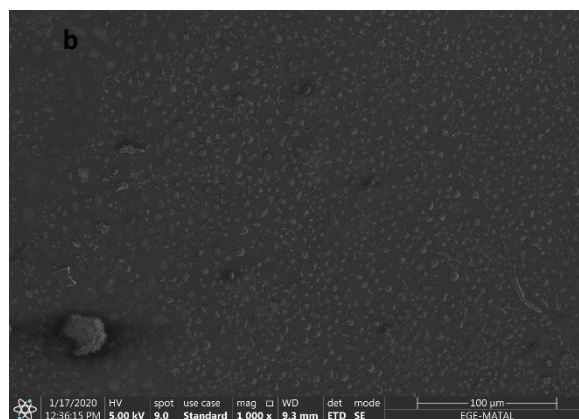
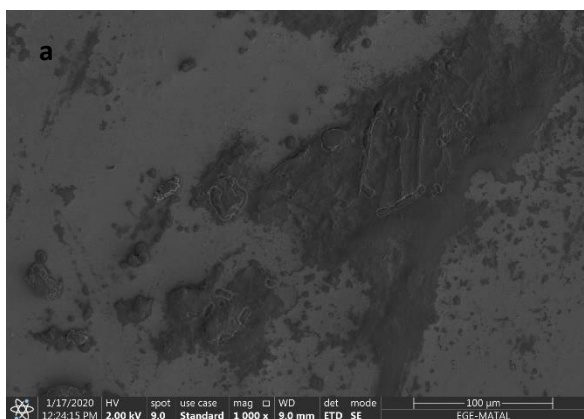


Figure 0.8: SEM morphological features (a) PEC-A (b) PEC-B (c) PEC-C (d) PEC-D (e) PEC-E at 100μm

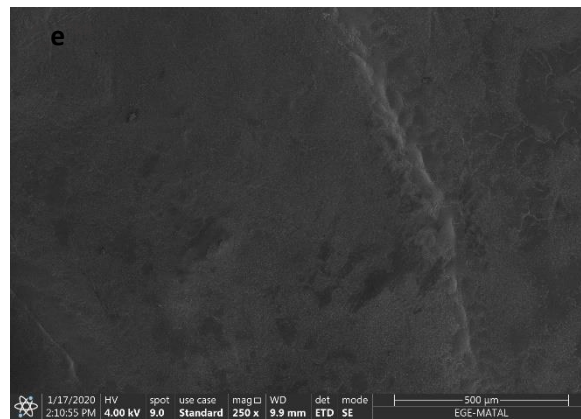
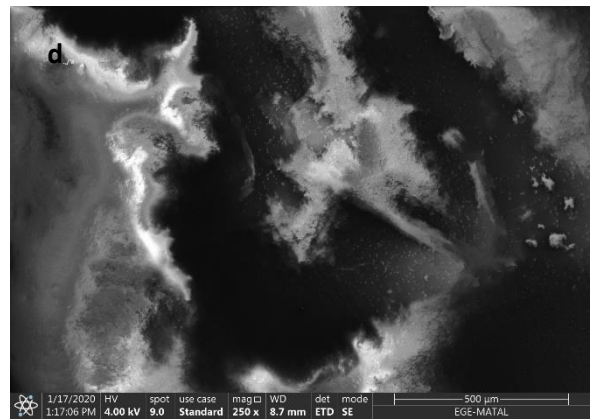
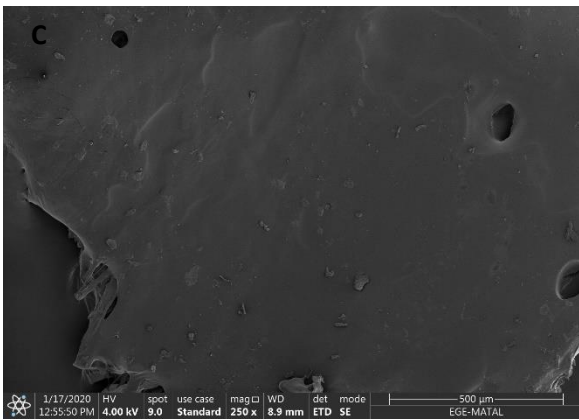
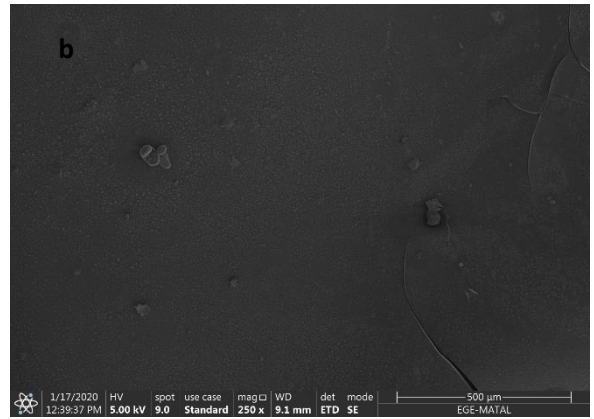
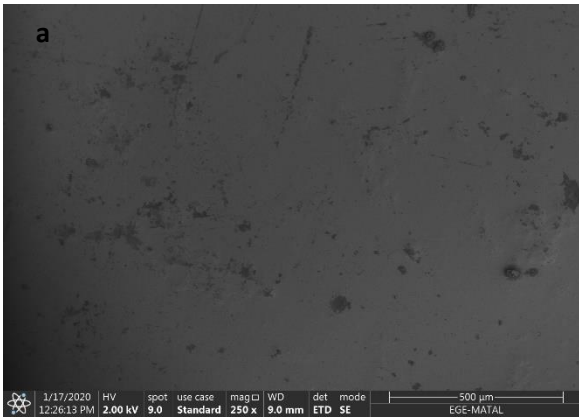


Figure 0.9: morphological features (a) PEC A (b) PEC B (c) PEC C (d) PEC D (e) PEC E at 500 μ m

Morphological study of clopidogrel bisulfate bilayer and trilayer PECs were studied using an electron scanning microscope (SEM) as shown in figure 4.5 to figure 4.9 at different microscopic scales 10 μ m, 20 μ m, 50 μ m, 100 μ m and 500 μ m respectively.

The SEM pictures of PEC-A are given in Figure 4.5 a to Figure 4.9 a respectively. In

Figure 4.5 a the drug loaded CHI-SF-CHI polyelectrolyte complex trilayer exhibited a rough surface with clopidogrel bisulphate particles cohering onto the surface of the film. Figure 4.6 a) and Figure 4.9 displayed a smooth heterogenous surface, however, SEM images Figure 4.7 a) and Figure 4.8 a) zoomed in at 50 μ m, 100 μ m respectively and displayed a heterogenous surface with roughness and surface cracks on the darker areas because of the biochemical stress during dehydration of the film.

A microscopic examination of the drug loaded SF-CH films provided information about the heterogeneity of the sample at 10 μ m and also showing polymer particles of the outer layer clustered sporadically onto the first layer. Figure 4.6 b) at 20 μ m clearly presented a rough cluster of the outer polymer layer particle adhered onto the smooth inner layer film. Images of PEC-B taken at 50 μ m and 100 μ m indicated porous rough matrices. Figure 4.9 a) displayed nanoparticles of clopidogrel bisulphate adhered onto the smooth homogenous part of the film.

The SEM photographs of PEC-C in Figure 4.5 c) show a rough, irregular outer layer studded with shiny white particles of the anticoagulant agent on a cracked heterogenous surface.

Figure 4.6 c and Figure 4.7 c show an extended crack while still exhibiting cluster of the outer layer. Figure 4.8 c and Figure 4.9 c register dispersed pores. A wrinkled outer layer was observed

The alginate, silk fibroin and chitosan composite PEC-D in figures 4.5 d) to 4.7 d) displayed a clustered outer layer morphology with a rough surface and ridges with minimal porosity. The micrograph of shown in figure 4.9 d) clearly shows the heterogeneity of the complex, the surface shows a dark pigment of grey, a lighter undertone in dispersed areas and shiny white opulence.

In all magnifications used PEC-E displayed the best distribution of composite because no outer layer clustering was observed.

PEC-B constructs highlighted a heterogenous structure due to their bilayer assimilation of SF-CHI composites. The films displayed so-called sea-island morphology, in comparison to PEC-

A and PEC-C, PEC-B the topography of PEC-A has a direct relation to the smaller clusters of the chitosan layer as a result of its non-homogeneity during the drying phase.

In contrary, all PECs showed minimal pore dispersion which may be a reason for the low cell viability. When comparing PEC-C and PEC-E, both films exhibited nanoclustering of outer layers, an observation can be made that PEC-D has a surface smoother than all when compared to the others, this may be a factor of why PEC-C exhibited the least cell viability in the cytotoxicity experiment

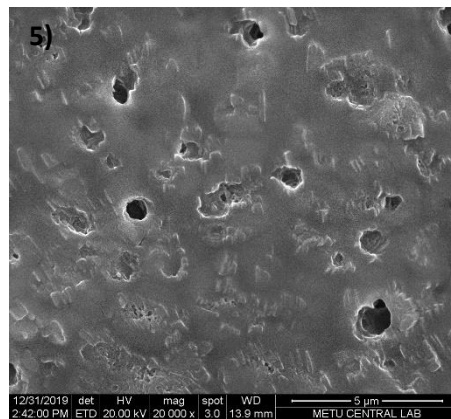
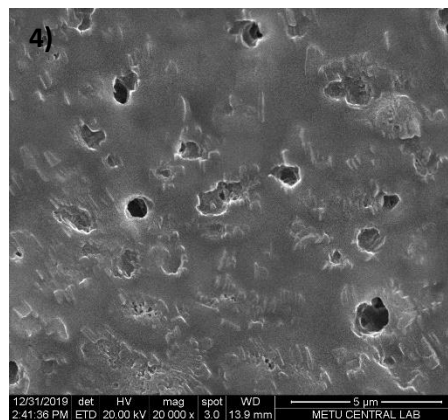
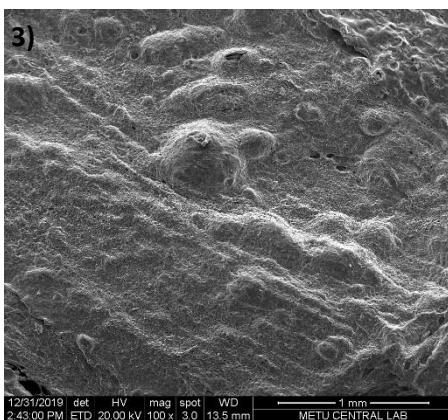
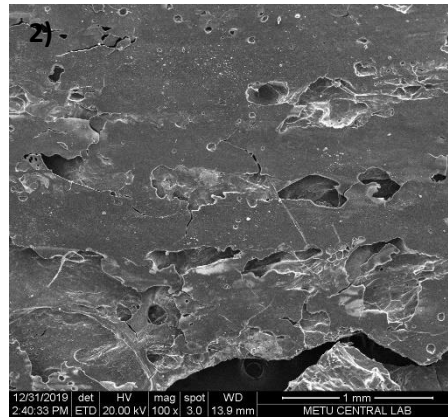
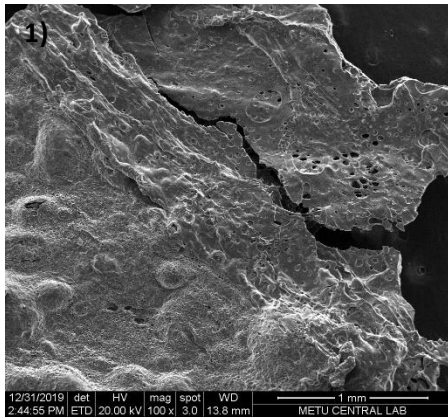


Figure 0.10: SEM micrographs showing morphological features of (1) PEC 1
 (2) PEC 2 (3) PEC 3 (4) PEC 4 (5) PEC 5 at 1mm

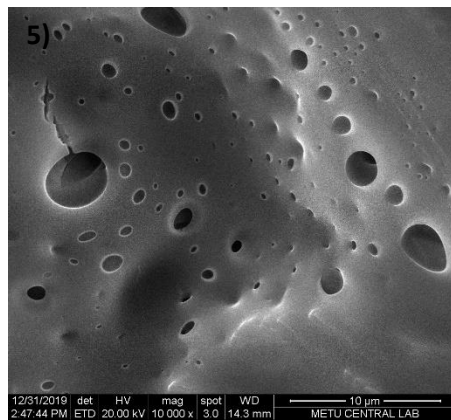
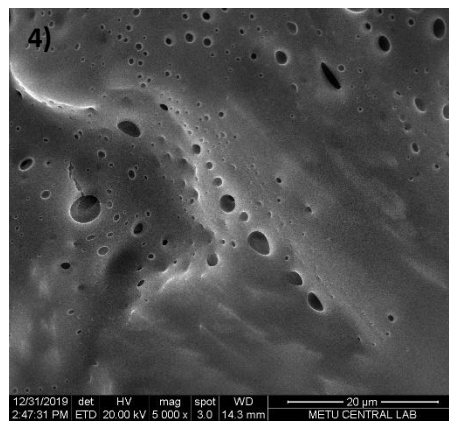
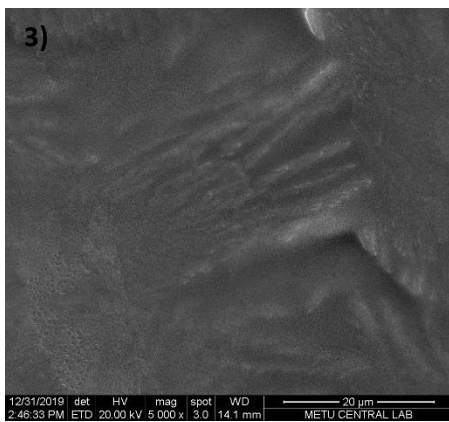
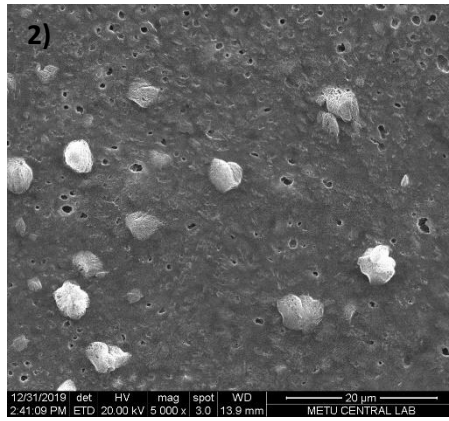
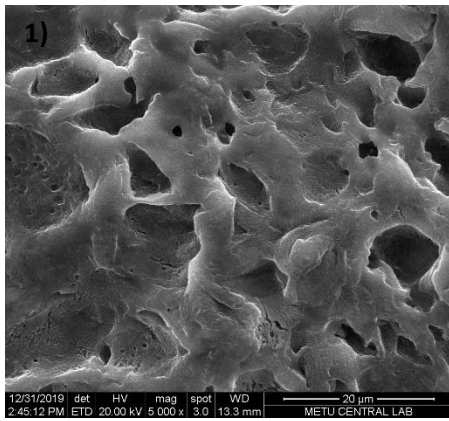


Figure 0.11: SEM micrographs showing morphological features of (1) PEC 1 (2) PEC 2 (3) PEC 3 (4) PEC 4 (5) PEC 5 at 20 μ m

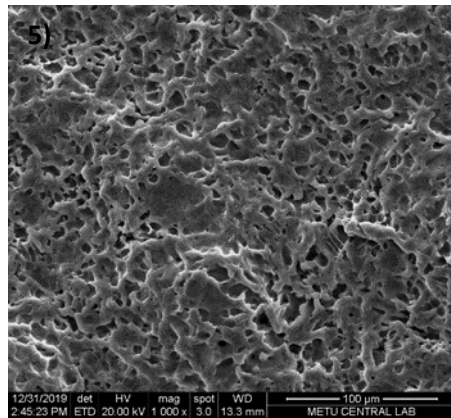
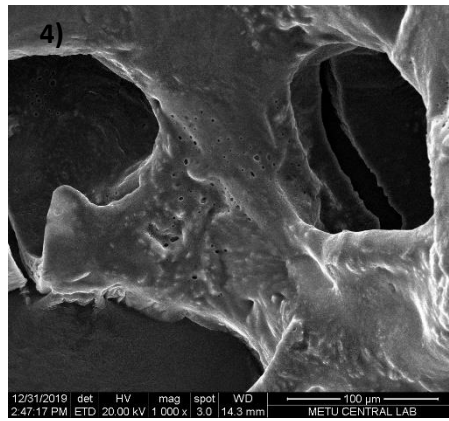
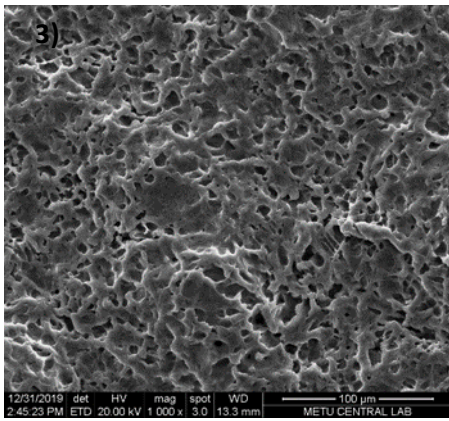
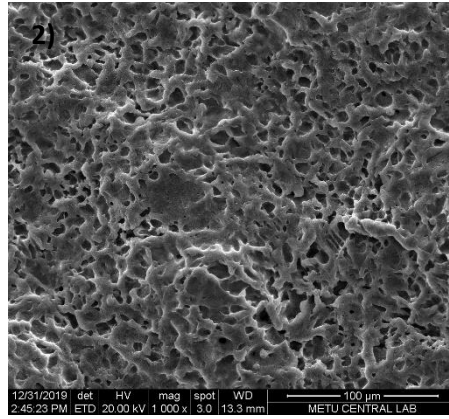
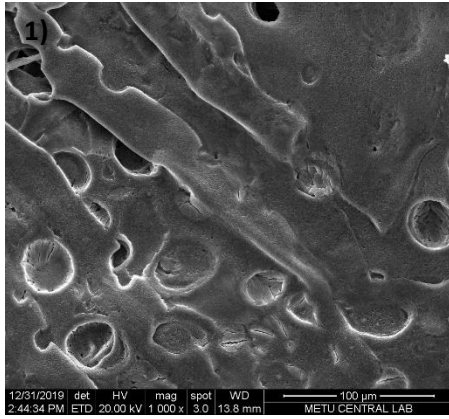


Figure 0.12: SEM micrographs showing morphological features of (1) PEC 1 (2) PEC 2 (3) PEC 3 (4) PEC 4 (5) PEC 5 at 100 μ m

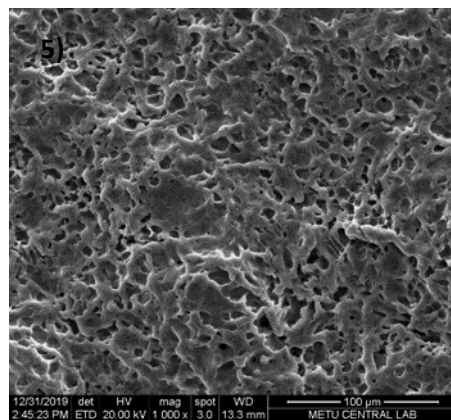
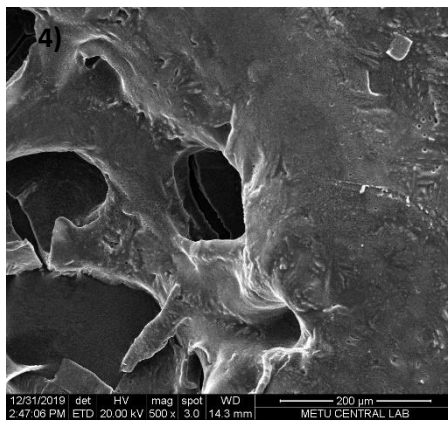
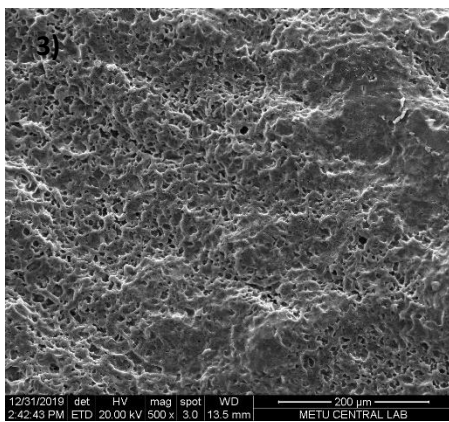
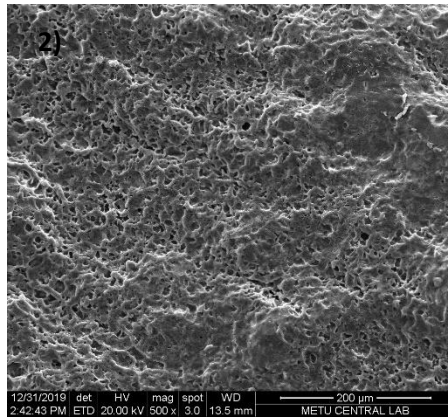
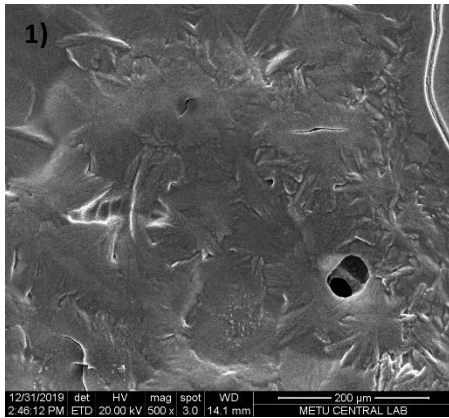


Figure 0.13: SEM micrographs showing morphological features (1) PEC 1 (2) PEC 2 (3) PEC 3 (4) PEC 4 (5) PEC 5 at 200 μ m

Additionally, morphologies of drug-free bilayer and trilayer PEC blends PECs were studied using an electron scanning microscope (SEM) as shown in figure 4.10 to figure 4.13 at selected microscopic scales 1mm, 20 μ m, 100 μ m, 200 μ m respectively.

At 1mm PEC-1 a CHI-SF-CHI polyelectrolyte complex trilayer displayed a rough surface that is sporadically porous. Figure 4.11 1) and Figure 4.13 1) present a surface with hollow perforations, images of the heterogenous blend seem dense and rough. Figure 4.12 1) shows dents on the surface of the film

PEC-2, a bilayer cast with a silk fibroin and chitosan outer layer SF-CH films provided information about the intense porosity of the sample. at 1mm the surface seems to have a rough overcast with dispersed cracks and dents, however as the magnification increased the sense dispersion of pores is were seen on the polymer. This micrograph confirms that the silk fibroin and chitosan interactions during solvent casting enhances pore formation.

Alike to micrographs of PEC-2, from low magnifications of 1mm and 20 μ m on PEC-3, the surface of this silk fibroin and chitosan tri-layer complex with SF as the outer layers seems to have a homogenous undertone from afar but as the magnification increases dissemination of closely packed pores increases as well.

The expanding porosity of composite films SF-CHI and SF-CH-SF which may relate to higher topological roughness, and high porosity which offers a more noteworthy cell adhesion factor.

The chitosan, silk fibroin and alginate composite PEC-4 in figures 4.10 4) to 4.13 4) clearly displays a minimally rough surface with general smoothness and large, hollow, and loosely packed pores

In all magnifications used to study PEC-5, the complex displayed both large loosely packed pores and as the magnification increases it is evident that the complex also has e very dense dispersion of pores.

All PECs showed pore dispersion and this is attributed to the polymers natural properties and being synthesised drug free.

4.4. Differential scanning calorimetry (DSC).

Table 4.2: DSC analysis of CLB loaded PECs where T_c °C - Exothermic Crystallization Peaks, T_M °C – Temperature Time Melting Point and T_D

SAMPLE	COMPOSITION	T_c °C	T_M °C	T_D °C	COMMENTS
PEC-A	CHI + SF + CHI + Drug	30.29, 48.47 69.53, 74.78 276.77	72.04, 290.18	450 218	Broad exothermic crystallinity peaks are seen at 30.29°C, 48.47°C, 69.53°C, 74.78 °C and 276.77°C analogous to these peaks are enthalpies of 3.530J/g, 1.283J/g, 2.523J/g, 53.66J/g and 37.66J/g respectively. The lowest melting point is seen at 72.04 °C while the sharpest endothermic peak is observed at 290.18 °C, followed by a denaturation peak of 450 °C
PEC-B	SF + CHI + Drug	122.68, 247.25	130.15, 279.41	450 148.99	Two exothermic peaks of approximately 122.68°C and 247.25°C thromboplastin observed with associated peak enthalpies of 169.3J/g and 97.58J/g respectively. Two distinct temperature time melting points are shown at 130.15°C and 279.41°C, followed by an expected decomposition peak marked at 450 °C
PEC-C	SF + CHI + SF + Drug	44.41, 253.62	83.31, 287.50	450 204.19	Exhibited two exothermic peaks, one being the weakest crystallinity peak at 44.41°C but the following peak appears to be one of the strongest at 253.62 °C. Correlated are enthalpy peaks of 140.9J/g and 195.3J/g individually. The thermograph additionally Gives two characteristic melting peaks of 83.31°C and 287.50 °C followed by a 450°C degradation peak.
PEC-D	AL + SF + CHI + Drug	44.61, 251.74	101.26, 277.89	450 176.63	Presents two pronounced exothermic crystallinity peaks at 44.61°C and 251.74°C, kindred by an enthalpy of 216.3J/g and 215.6J/g respectively. Two temperature time melting points were observed at 101.26 °C and 277.89 °C and denatured at 450 °C
PEC-E	AL + SF + AL + Drug	44.71, 255.75	101.92, 278.14	450 176.22	Displays two exothermic peaks, one at 44.71°C associated with an enthalpy of 464.0J/g and the second peak exhibiting the highest crystallinity peak at 255.75°C with a 193.3J/g enthalpy. Two temperature time melting points were observed at 101.92 °C and 278.14 °C and were denatured at 450 °C

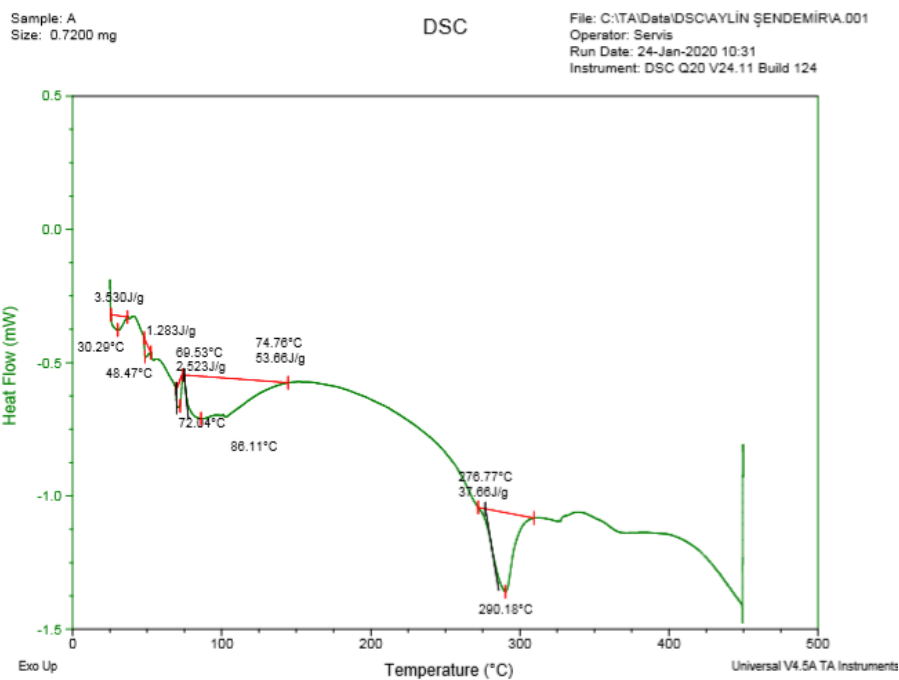


Figure 0.14: DSC thermogram of PEC-A

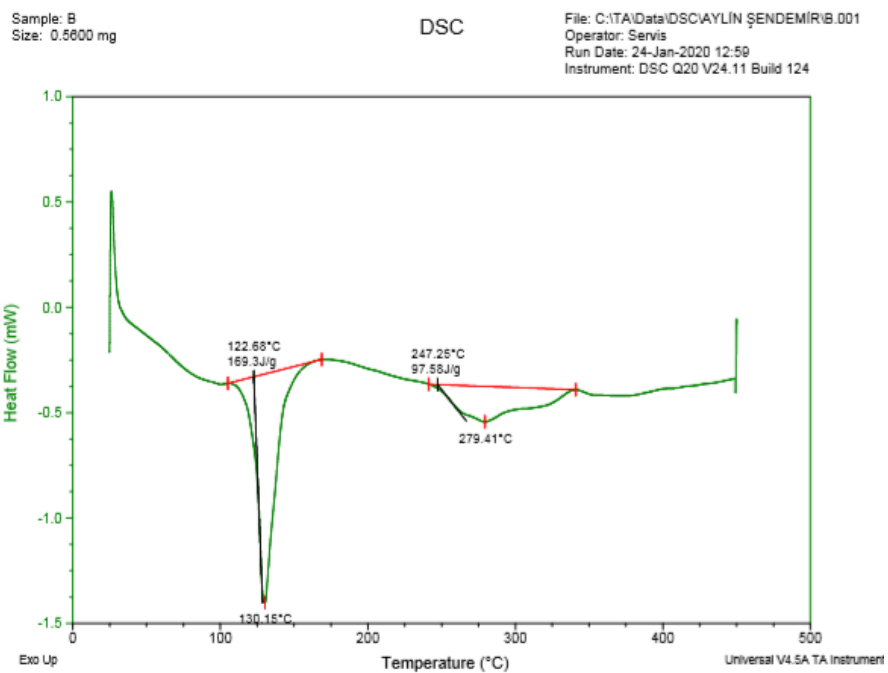


Figure 0.15: DSC thermogram of PEC-B

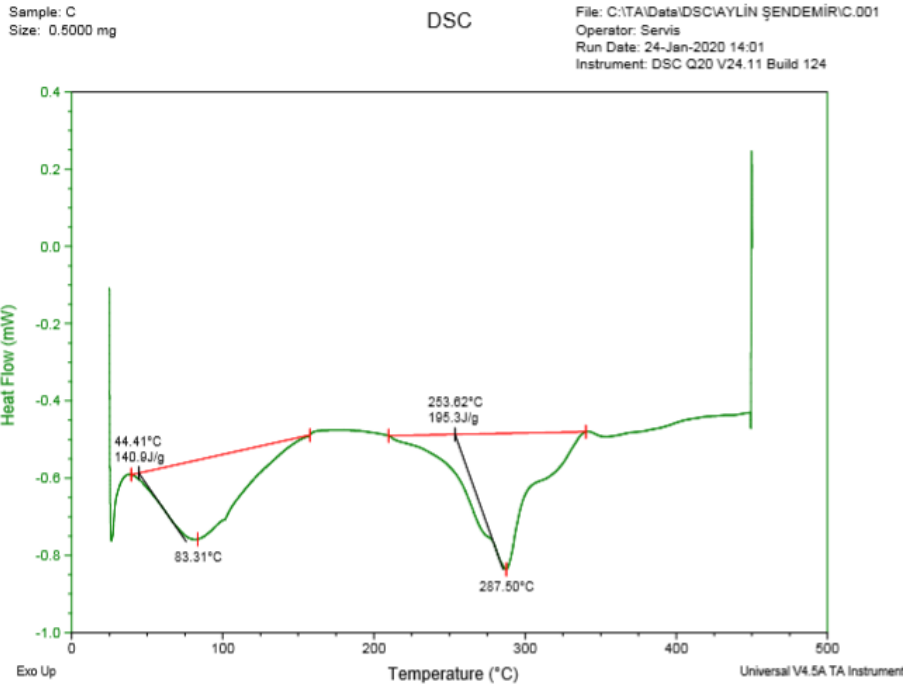


Figure 0.16: DSC thermogram of PEC-C

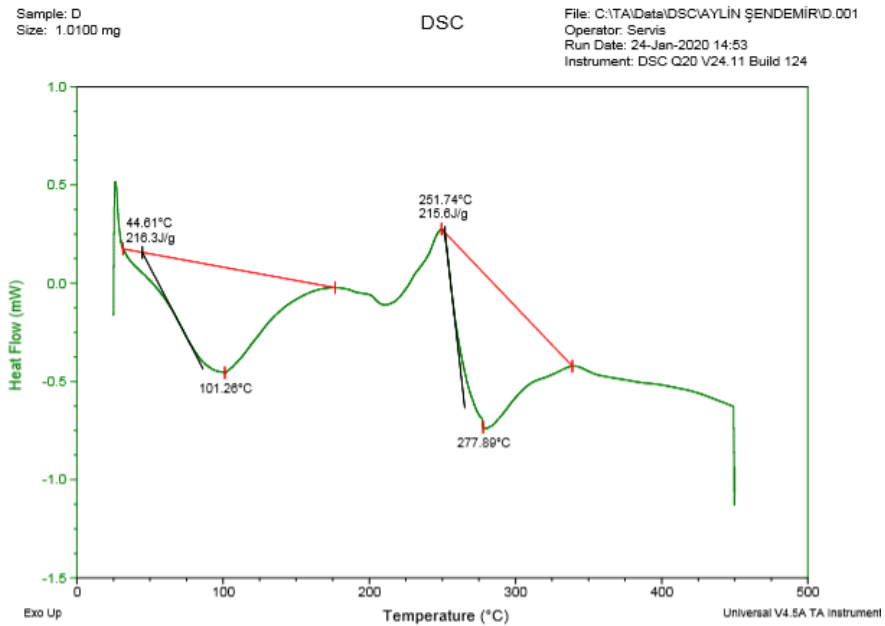


Figure 0.17: DSC thermogram of PEC-D

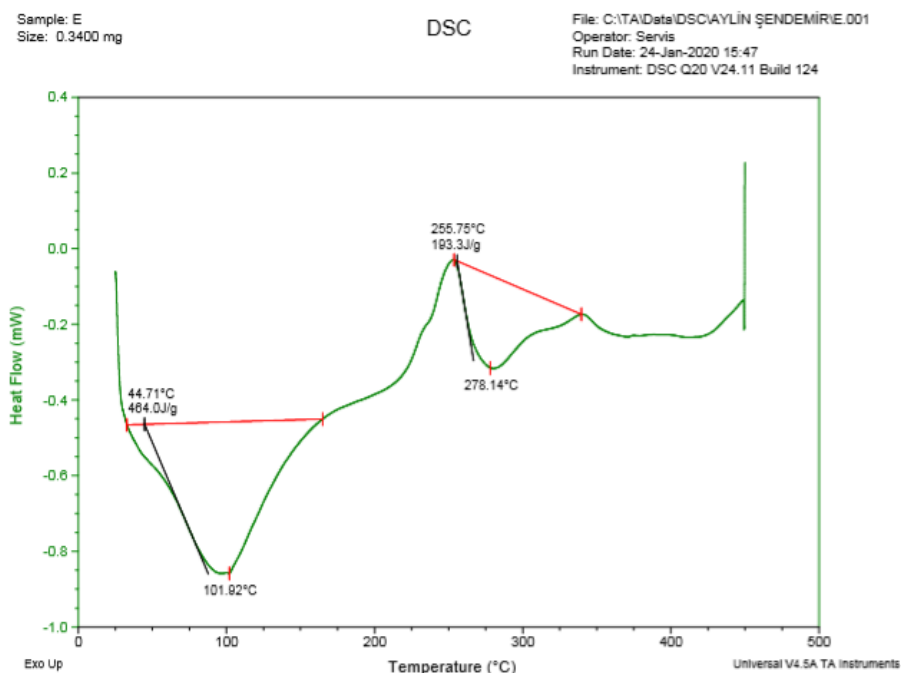


Figure 0.18: DSC thermogram of PEC-E

An analysis of the DSC thermograms of samples PEC_A, PEC_B, PEC_C, PEC_D, and PEC_E are shown in the tables above. As can be seen PEC-A has five exothermic crystallinity peaks shown at 30.29°C, 48.47°C, 69.53°C, 74.78 °C and 276.77°C, the multiple increasing crystallinity peaks are due to evaporation of moisture from the trilayer CHI-SF-CHI complex. Chitosan is composed of rigid molecular chains, nanofibrils, and nanofibril clusters so in the highest volume of chitosan used in all PECs the effect results in multiple crystallinity peaks.

As seen, PEC-C, PEC-D and PEC-E exhibited relatively double peaked patterns, low initial endothermic peaks at 44.41°C, 44.61°C, 44.71°C and the maximum crystallinity occurs at 253.62°C, 251.74°C and 255.75°C respectively, demonstrating the exposure of hydrophilic groups in PECs that have turned out to be progressively presented likely because of the arrangement of more interstices in the wake of complexing.

It is evident from this data that polymer complex PEC-A registers the best thermal stability shown by the largest difference in exothermic peaks 72.04°C, 290.18°C among all the samples, indicating stronger interaction between chitosan and silk fibroin trilayer formation. This might be brought about by progressively accessible protonated amine groups in

chitosan for response with carboxylic groups in silk fibroin. PEC-B indicated the weakest thermal stability, registered by the least difference in exothermic peaks 130.15°C and 279.41°C respectively among all the, An indication of oxidative degradation and hydrogen bonding disruption due to loss of free amine groups.

PEC-D and PEC-E exhibited very similar exothermic and endothermic peaks, the difference is due to the difference in the third outer layer and the maximum thermal decomposition rate occurs around 450 °C for all poly electrolyte complexes

4.5. Atomic force microscopy (AFM)

Influence of AFM operating modes on clopidogrel bisulphate loaded PECS morphology is illustrated in figures 4.10 to 4.14 and table 4.13 shows the root mean square roughness (Ra), PEC thickness (Z) and numerical median of the PEC absolute exterior and width variations estimated from its standard PEC plane (Ra).

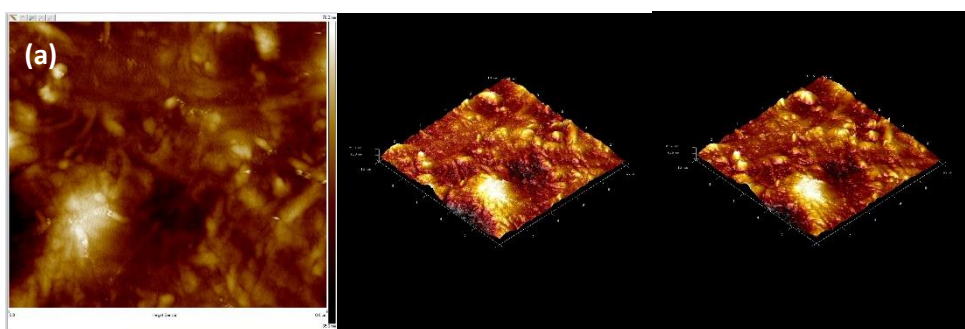


Figure 0.19: AFM results of PEC-A

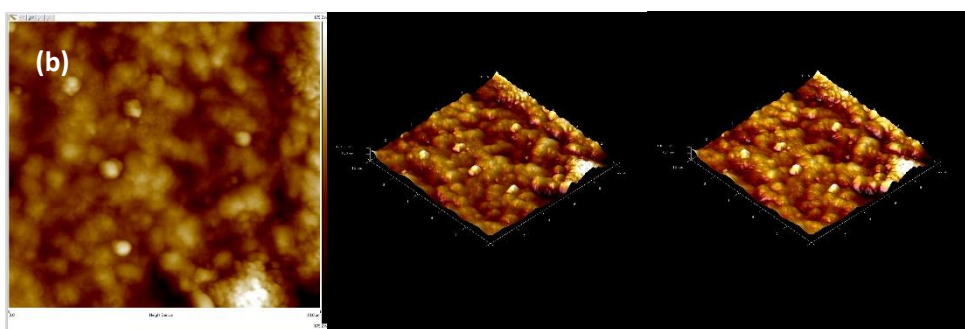


Figure 0.20: AFM results of PEC-B

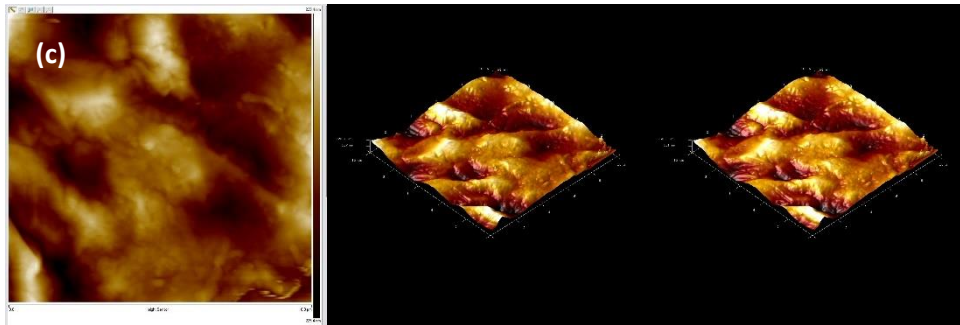


Figure 0.21: AFM results of PEC-C

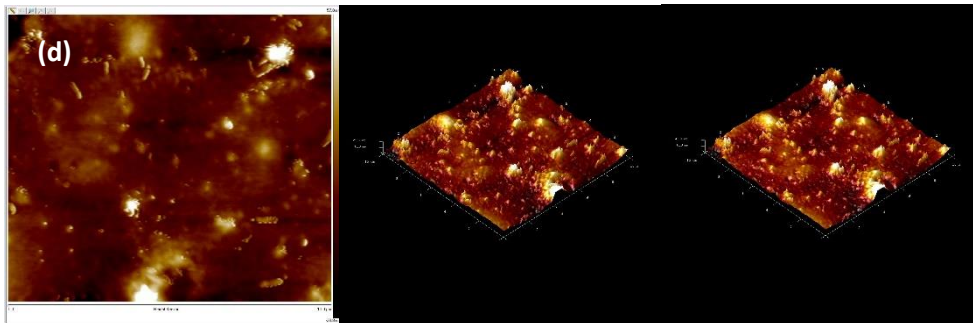


Figure 0.22: AFM results of PEC-D

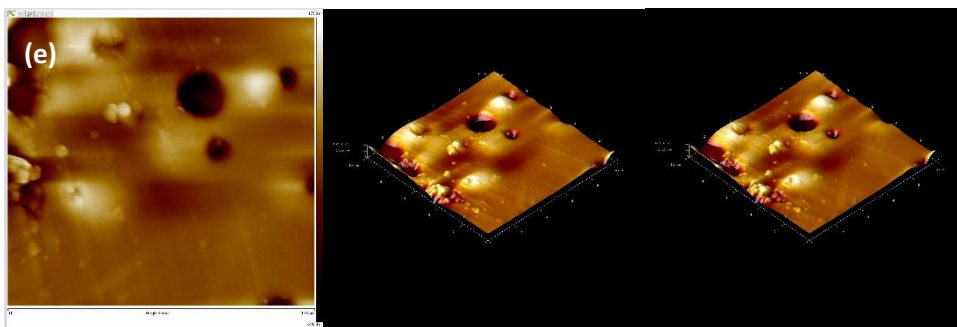


Figure 0.23: AFM results of PEC-E

Table 4.3: Properties of PECs measured by AFM.

Samples	Z(μm)	Root mean square roughness R_{rms} (μm)	Image Ra (μm)
PEC-A	0.154	0.0177	0.0131
PEC-B	0.395	0.0448	0.0342
PEC-C	0.436	0.0665	0.0536
PEC-D	0.167	0.0121	0.00806
PEC-E	0.411	0.0444	0.0292

Topographic features present PEC-A, a trilayer composite of CHI-SF-CHI to have the least thickness of $0.154\mu\text{m}$, while PEC-C, a trilayer composite of SF-CHI-SF has the most PEC thickness of $0.436\mu\text{m}$. Generally, the smoothness or roughness of the outer most layers of the membranes affects the thickness of the film, rotating it with SF, CHI or AL has shown to have an impact on the morphology of the film.

In this study, the number of layers had no bearing on the thickness of the film, it was all dependant on the drying characteristics of the outer most layers. The surface roughness of PEC-C is registered as $0.0665\mu\text{m}$, parallel to that is the highest Image Ra of $0.0536\mu\text{m}$.

The bright opulent parts of are attributed to the aggregation of clopidogrel bisulphate.

4.6.Cytotoxicity analysis

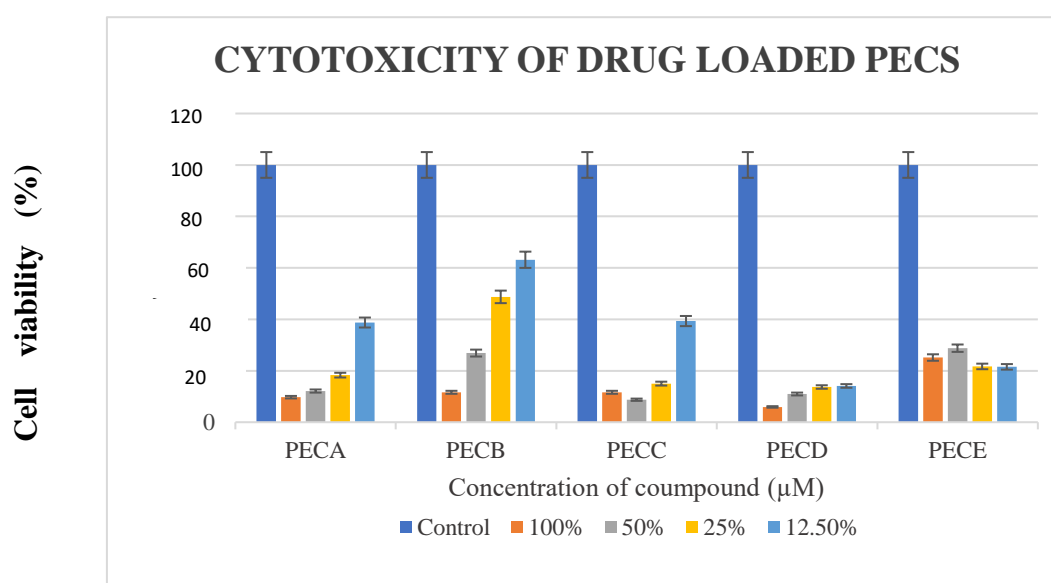


Figure 4.24: *In vitro* cytotoxic effect of PEC_A, PEC_B, PEC_C, PEC_D and PEC_E on cell viability.

All tests were repeated three times by using IBM SPSS Statistics (Version 24). Tukey was selected and The findings of one-way ANOVA study were evaluated using $p = 0.05$, *post-hoc* method. Cell viability results were below 70 % indicated that, PECs were cytotoxic according to the ISO 10993-5:2009 *In vitro* Cytotoxicity Test standards. Different from other A, C, D, and E samples, 25 % and 12.5 % extraction concentrations of sample B were less cytotoxic than other samples.

Shown are unsatisfactory results of the cell proliferation in a concentration dependant way that was perpetually hindered. As seen in the graph above, the various polyelectrolyte complexes show an adverse influence on cell viability.

Percentage viability of cells grown and monitored on these PEC films was not of standard statistical validity. Although the synthesized complexes proved to have cytotoxic properties for the cell line, it is pertinent to mention that the used cells had the least growth inhibition on PEC-B.

In comparison to all other polyelectrolyte complexes the clopidogrel bisulfate loaded SF-CHI bilayer had a significantly higher degree of cell viability of 11.62%, 26.87%, 48.72% and 63.14% in 100%, 50%, 25% and 12.5% concentration of compound (μM) respectively. Particularly, PEC-D exhibited the strongest cytotoxic effect *in vitro* against the cells as illustrated in the graph by having the lowest cell viability however PEC-A, PEC-C and PEC-E showed relatively low cell viabilities as well.

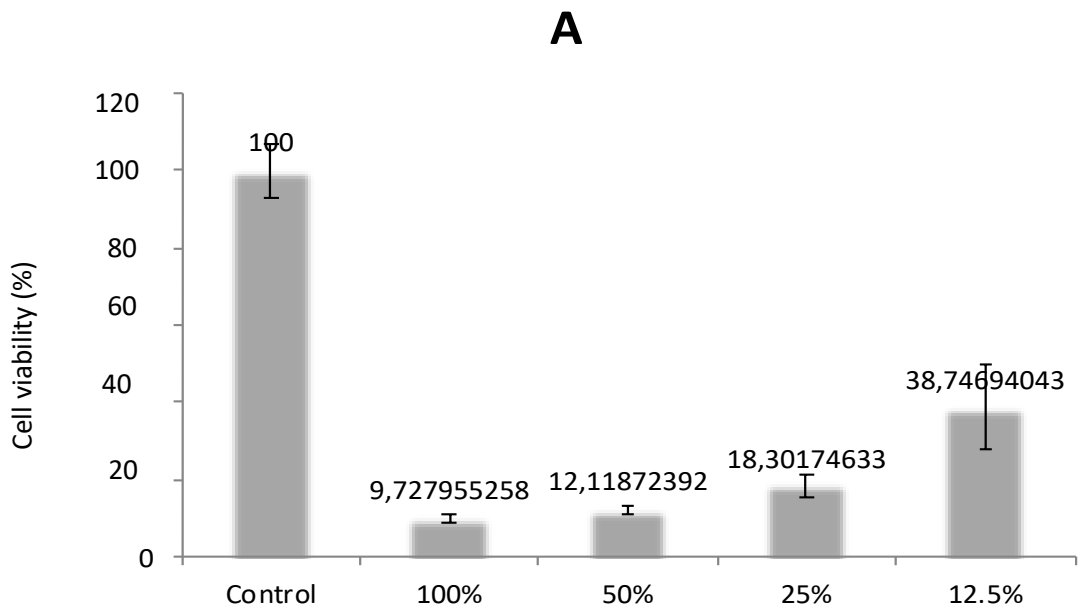


Figure 0.25: Concentration dependent *in vitro* cytotoxic effect of PEC-A

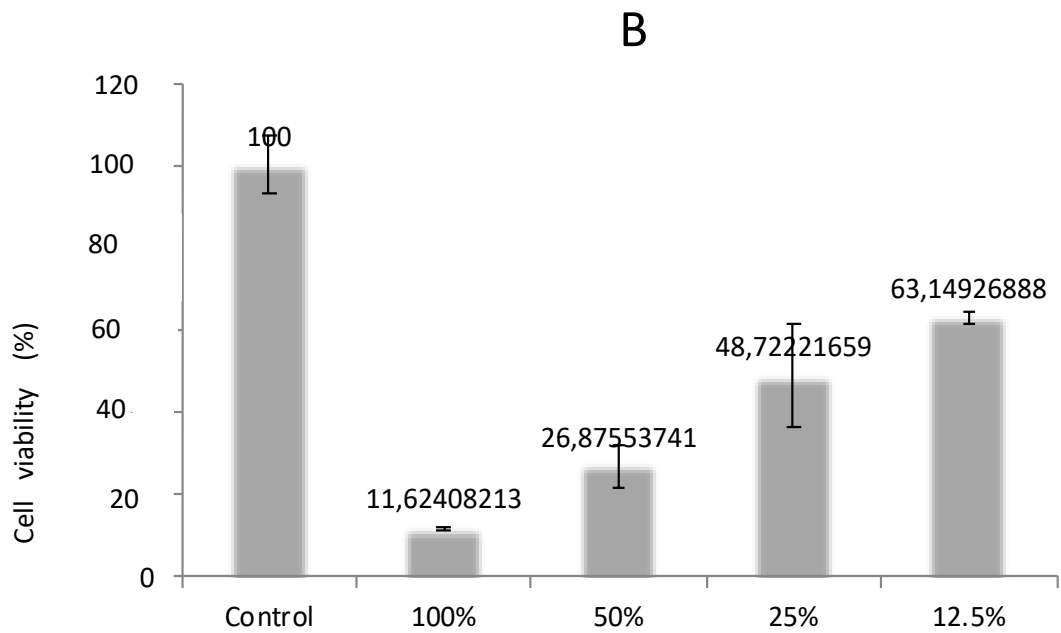


Figure 0.26: Concentration dependent *in vitro* cytotoxic effect of PEC-B

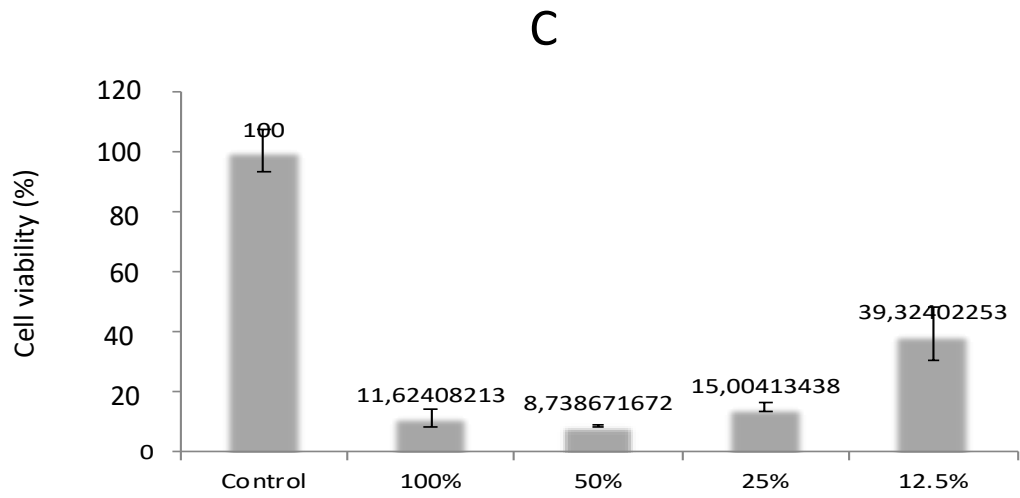


Figure 0.27: Concentration dependent *in vitro* cytotoxic effect of PEC-C

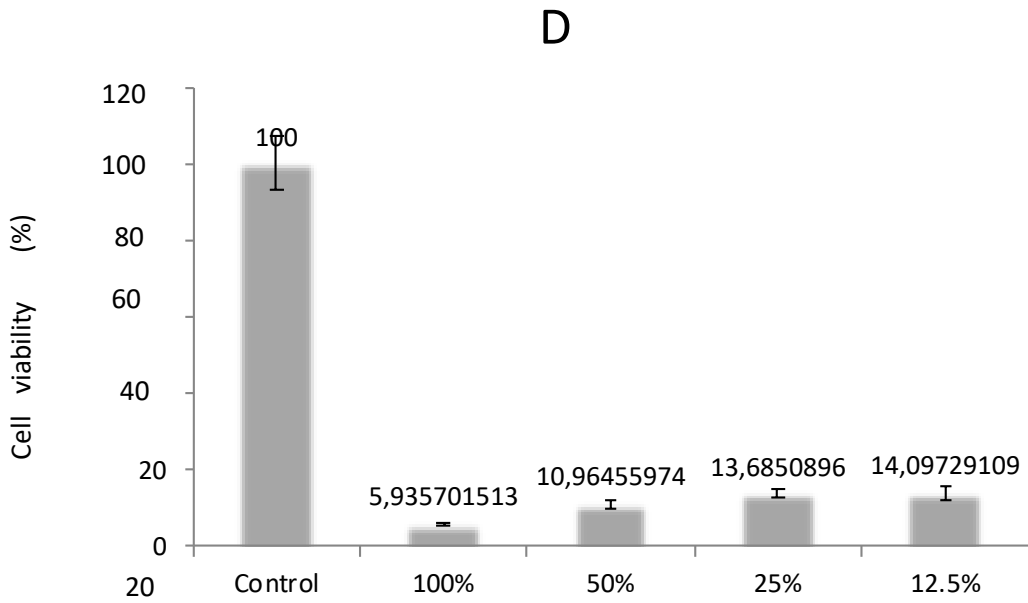


Figure 0.28: Concentration dependent *in vitro* cytotoxic effect of PEC-D

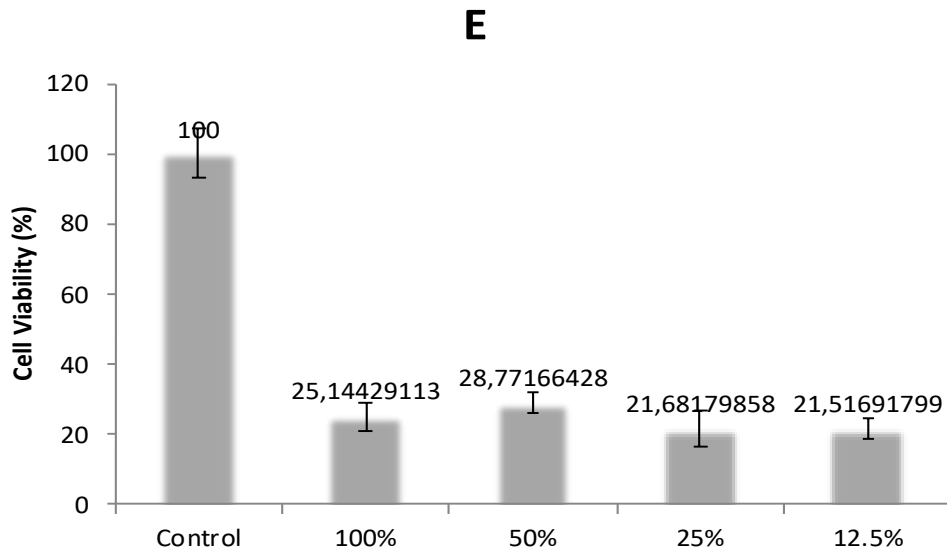


Figure 0.24: Concentration dependent *in vitro* cytotoxic effect of PEC-E

4.7.PT, INR & APTT

The compatibility of the LbL PECs with fresh human venous blood was investigated (Table 4.4). Normal range for PT is 11 to 13.5 seconds (Adcock & Gosselin, 2017), the regular healthy weight range for APTT is between 30 and 40 seconds however if the material has an antithrombogenic agent then the expected range is between 120 and 140 seconds (Adcock & Gosselin, 2017). In healthy people the threshold value for INR is considered to be 1.1. Patients taking antithrombogenic medication generally offer a range of 2.0 to 3.0 (Adcock & Gosselin, 2017).

Table 4.4: In-vitro coagulation test analysis results.

Sample	PT (%)	PT (Seconds)	INR (Seconds)	APTT (Seconds)
PEC-1	85	14.2	1.12	29.2
PEC-3	54	19.5	1.57	194.4
PEC-E	76	15.52	1.20	32.5
HM- Healthy Blood	91	13.6	1.07	31.0

4.8.Total cholesterol test

Cholesterol efflux from cholesterol-labelled venous blood to Fatty acid-free human serum albumin (HSA) is multi - factorial with a rapid early phase that peaks at about 15 minutes followed by an almost sequential phase of up to 90 min. Cholesterol efflux saturation was ascertained to approximately 182 mg / dL (Table 4.5). In a healthy adult the quintessential cholesterol range is below 170mg / dL.

Table 4.5: Total cholesterol test results.

Sample	Total Cholesterol
PEC-1	182mg/dL

4.9.Albumin test

The extent measurement of surface binding of albumin to the tri-Layer PEC film CH-SF-CH was recorded as 4.8g/dL which was within the normal range. For a healthy adult the average albumin level is 3.4 g /dL to 3.56 g /dL.

Table 4.6: Albumin test results.

Sample	Albumin
PEC-1	4.8g/dL

CONCLUSION

The silk fibroin, chitosan and alginate materials have been successfully used to prepare polyelectrolyte complexes. Characterization of the PECs was performed by using AFM, DSC and SEM. The results indicated that, PECs having two or three layers on a polyelectrolyte complex film has no bearing on the film thickness but the dehydration properties of the outer most layer does. The increasing crystallinity peaks have differences in exothermic peaks. The results from the DSC analysis suggested that PECs with SF and CHI interactions with the chitosan as an outer layer possesses the best thermal stability. In this study, the PECs of different layer-by-layer design can integrate and form PECs with favourable swelling kinetics, thermal degradation and non-thrombogenicity. Although the polyelectrolyte complexes exhibited high cytotoxicity, the PECs have promising potential of being improved and eventually being used in biomedical applications if toxicity is eliminated and properties are improved. For future works, this study may be improved by crosslinking with TPP/MBA or incorporating other polyelectrolyte complexes such as curcumin or gelatin to improve cell-surface adhesion. Use of LbL casting has proven to have an effective technique on the surface morphology of the films.

REFERENCES

- Adali, T., & Uncu, M. (2013). Non-thrombogenic silk fibroin-graft-poly(tri(ethylene glycol dimethacrylate) biofilms. *Current Opinion in Biotechnology*, *24*, S47. <https://doi.org/10.1016/j.copbio.2013.05.109>
- Adali, T., & Yilmaz, E. (2009). Synthesis, characterization and biocompatibility studies on chitosan-graft-poly(EGDMA). *Carbohydrate Polymers*, *77*(1), 136–141. <https://doi.org/10.1016/j.carbpol.2008.12.017>
- Adcock, D. M., & Gosselin, R. C. (2017). The danger of relying on the APTT and PT in patients on DOAC therapy, a potential patient safety issue. *International Journal of Laboratory Hematology*, *39*(January), 37–40. <https://doi.org/10.1111/ijlh.12658>
- Alshhab, A., & Yilmaz, E. (2019). Sodium alginate/poly(4-vinylpyridine) polyelectrolyte multilayer films: Preparation, characterization and ciprofloxacin HCl release. *International Journal of Biological Macromolecules*. <https://doi.org/10.1016/j.ijbiomac.2019.10.058>
- Azizur Rahman, M. (2019). Collagen of extracellular matrix from marine invertebrates and its medical applications. *Marine Drugs*, *17*(2), 1–12. <https://doi.org/10.3390/md17020118>
- Bahramzadeh, E., Yilmaz, E., & Adali, T. (2019). Chitosan-graft-poly(N-hydroxy ethyl acrylamide) copolymers: Synthesis, characterization and preliminary blood compatibility in vitro. *International Journal of Biological Macromolecules*, *123*, 1257–1266. <https://doi.org/10.1016/j.ijbiomac.2018.12.023>
- Behera, S. S., Das, U., Kumar, A., Bissoyi, A., & Singh, A. K. (2017). Chitosan/TiO₂ composite membrane improves proliferation and survival of L929 fibroblast cells: Application in wound dressing and skin regeneration. *International Journal of Biological Macromolecules*, *98*, 329–340. <https://doi.org/10.1016/j.ijbiomac.2017.02.017>
- Bushkalova, R., Farno, M., Tenailleau, C., Duployer, B., Cussac, D., Parini, A., ... Girod Fullana, S. (2019). Alginate-chitosan PEC scaffolds: A useful tool for soft tissues cell therapy. *International Journal of Pharmaceutics*, *571*, 118692. <https://doi.org/10.1016/j.ijpharm.2019.118692>
- Coquery, C., Carosio, F., Negrell, C., Caussé, N., Pébère, N., & David, G. (2019). New bio-based phosphorylated chitosan/alginate protective coatings on aluminum alloy obtained by the LbL technique. *Surfaces and Interfaces*, *16*(April), 59–66. <https://doi.org/10.1016/j.surfin.2019.04.010>
- Daristotle, J. L., Lau, L. W., Erdi, M., Hunter, J., Djoum, A., Srinivasan, P., ... Kofinas, P. (2019). Sprayable and biodegradable, intrinsically adhesive wound dressing with antimicrobial properties. *Bioengineering & Translational Medicine*. <https://doi.org/10.1002/btm2.10149>
- Dekoninck, S., & Blanpain, C. (2019). Stem cell dynamics, migration and plasticity during wound healing. *Nature Cell Biology*, *21*(1), 18–24. <https://doi.org/10.1038/s41556-018-0237-6>
- Desai, N., & Purohit, R. (2017). Development of Novel High Density Gastroretentive Multiparticulate Pulsatile Tablet of Clopidogrel Bisulfate Using Quality by Design Approach. *AAPS PharmSciTech*, *18*(8), 3208–3218. <https://doi.org/10.1208/s12249-017-0805-2>
- Gierszewska, M., Ostrowska-Czubenko, J., & Chrzanowska, E. (2018). pH-responsive

- chitosan/alginate polyelectrolyte complex membranes reinforced by tripolyphosphate. *European Polymer Journal*, *101*(November 2017), 282–290.
<https://doi.org/10.1016/j.eurpolymj.2018.02.031>
- Han, Y., Li, X., Zhang, Y., Han, Y., Chang, F., & Ding, J. (2019). Mesenchymal Stem Cells for Regenerative Medicine. *Cells*, *8*(8), 886.
<https://doi.org/10.3390/cells8080886>
- Hatami, J., Silva, S. G., Oliveira, M. B., Costa, R. R., Reis, R. L., & Mano, J. F. (2017). Multilayered films produced by layer-by-layer assembly of chitosan and alginate as a potential platform for the formation of human adipose-derived stem cell aggregates. *Polymers*, *9*(9), 1–13. <https://doi.org/10.3390/polym9090440>
- Hubbe, M. A., Rojas, O. J., & Lucia, L. A. (2015). Surface modification: Review. *BioResources*, *10*(3), 6095–6206. Retrieved from www.consumerreports.org
- Ishihara, M., Kishimoto, S., Nakamura, S., Sato, Y., & Hattori, H. (2019). Polyelectrolyte complexes of natural polymers and their biomedical applications. *Polymers*, *11*(4), 1–12. <https://doi.org/10.3390/polym11040672>
- Izumrudov, V. A., Mussabayeva, B. K., Kassymova, Z. S., Klivenko, A. N., & Orazzhanova, L. K. (2019). Interpolyelectrolyte complexes: advances and prospects of application. *Russian Chemical Reviews*, *88*(10), 1046–1062.
<https://doi.org/10.1070/rcr4877>
- Kim, M. S., Song, H. J., Lee, J., Yang, B. R., Choi, N. K., & Park, B. J. (2019). Effectiveness and Safety of Clopidogrel Co-administered With Statins and Proton Pump Inhibitors: A Korean National Health Insurance Database Study. *Clinical Pharmacology and Therapeutics*, *106*(1), 182–194. <https://doi.org/10.1002/cpt.1361>
- Kiziltay, A., Gündoğan, Z., Erel-göktepe, İ., & Hasirci, N. (2019). *Multilayer polymeric films for controlled release of ceftriaxone sodium Ceftriaxone sodyumun kontrollü salımı için çok katmanlı polimerik filmler*. *76*(3), 303–312.
- Krishtul, S., Baruch, L., & Machluf, M. (2019). Processed Tissue-Derived Extracellular Matrices: Tailored Platforms Empowering Diverse Therapeutic Applications. *Advanced Functional Materials*, *1900386*, 1–26.
<https://doi.org/10.1002/adfm.201900386>
- Landry, M. J., Gu, K., Harris, S. N., Al-Alwan, L., Gutsin, L., De Biasio, D., ... Barrett, C. J. (2019). Tunable Engineered Extracellular Matrix Materials: Polyelectrolyte Multilayers Promote Improved Neural Cell Growth and Survival. *Macromolecular Bioscience*, *19*(5), 1–11. <https://doi.org/10.1002/mabi.201900036>
- LeBleu, V. S., & Kalluri, R. (2018). A peek into cancer-associated fibroblasts: Origins, functions and translational impact. *DMM Disease Models and Mechanisms*, *11*(4), 1–9. <https://doi.org/10.1242/dmm.029447>
- Li, D. W., He, J., He, F. L., Liu, Y. L., Liu, Y. Y., Ye, Y. J., ... Yin, D. C. (2018). Silk fibroin/chitosan thin film promotes osteogenic and adipogenic differentiation of rat bone marrow-derived mesenchymal stem cells. *Journal of Biomaterials Applications*, *32*(9), 1164–1173. <https://doi.org/10.1177/0885328218757767>
- López-García, J., Lehocký, M., Humpolíček, P., & Sáha, P. (2014). HaCaT Keratinocytes Response on Antimicrobial Atelocollagen Substrates: Extent of Cytotoxicity, Cell Viability and Proliferation. *Journal of Functional Biomaterials*, *5*(2), 43–57.
<https://doi.org/10.3390/jfb5020043>
- Meka, V. S., Sing, M. K. G., Pichika, M. R., Nali, S. R., Kolapalli, V. R. M., & Kesharwani, P. (2017). A comprehensive review on polyelectrolyte complexes. *Drug*

- Discovery Today*, 22(11), 1697–1706. <https://doi.org/10.1016/j.drudis.2017.06.008>
- Muzzio, N. E., Pasquale, M. A., Gregurec, D., Diamanti, E., Kosutic, M., Azzaroni, O., & Moya, S. E. (2016). Polyelectrolytes Multilayers to Modulate Cell Adhesion: A Study of the Influence of Film Composition and Polyelectrolyte Interdigitation on the Adhesion of the A549 Cell Line. *Macromolecular Bioscience*, 16(4), 482–495. <https://doi.org/10.1002/mabi.201500275>
- Nachimuthu, S., Sadhasivam, B., Veerichetty, V., Ponnusamy, R., Muthukumar, P., T, S., & priya, D. (2018). In Situ Synthesis of Silk Fibroin Mediated Silver Nanoparticles in Chitosan-PeO Film and Studies on Release Kinetics for Wound Dressing Application. *Journal of Chemical and Pharmaceutical Sciences*, 11(01), 35–39. <https://doi.org/10.30558/jchps.20181101007>
- Nawae, S., Meesane, J., Muensit, N., & Daengngam, C. (2018). PT Biological Materials for Medicine Research Unit (BMM), Institute of Biomedical. *Materials & Design*, #pagerange#. <https://doi.org/10.1016/j.matdes.2018.10.041>
- Pahal, S., Gakhar, R., Raichur, A. M., & Varma, M. M. (2017). Polyelectrolyte multilayers for bio-applications: recent advancements. *IET Nanobiotechnology*, 11(8), 903–908. <https://doi.org/10.1049/iet-nbt.2017.0007>
- Pappa, A. M., Inal, S., Roy, K., Zhang, Y., Pitsalidis, C., Hama, A., ... Owens, R. M. (2017). Polyelectrolyte Layer-by-Layer Assembly on Organic Electrochemical Transistors. *ACS Applied Materials and Interfaces*, 9(12), 10427–10434. <https://doi.org/10.1021/acsami.6b15522>
- Patil, S., & Singh, N. (2019). Antibacterial silk fibroin scaffolds with green synthesized silver nanoparticles for osteoblast proliferation and human mesenchymal stem cell differentiation. *Colloids and Surfaces B: Biointerfaces*, 176(December 2018), 150–155. <https://doi.org/10.1016/j.colsurfb.2018.12.067>
- Patrulea, V., Laurent-Applegate, L. A., Ostafe, V., Borchard, G., & Jordan, O. (2019). Polyelectrolyte nanocomplexes based on chitosan derivatives for wound healing application. *European Journal of Pharmaceutics and Biopharmaceutics*, 140(May), 100–108. <https://doi.org/10.1016/j.ejpb.2019.05.009>
- Scarritt, M., Murdock, M., & Badylak, S. F. (2019). Biologic Scaffolds Composed of Extracellular Matrix for Regenerative Medicine. In *Principles of Regenerative Medicine*. <https://doi.org/10.1016/b978-0-12-809880-6.00035-7>
- Srisuwan, Y., & Baimark, Y. (2013). Preparation of biodegradable silk fibroin/alginate blend films for controlled release of antimicrobial drugs. *Advances in Materials Science and Engineering*, 2013. <https://doi.org/10.1155/2013/412458>
- Sun, W., Chen, G., Wang, F., Qin, Y., Wang, Z., Nie, J., & Ma, G. (2018). Polyelectrolyte-complex multilayer membrane with gradient porous structure based on natural polymers for wound care. *Carbohydrate Polymers*, 181, 183–190. <https://doi.org/10.1016/j.carbpol.2017.10.068>
- Tu, H., Wu, G., Yi, Y., Huang, M., Liu, R., Shi, X., & Deng, H. (2019). Layer-by-layer immobilization of amphoteric carboxymethyl chitosan onto biocompatible silk fibroin nanofibrous mats. *Carbohydrate Polymers*, 210, 9–16. <https://doi.org/10.1016/j.carbpol.2019.01.047>
- Vizovišek, M., Fonović, M., & Turk, B. (2019). Cysteine cathepsins in extracellular matrix remodeling: Extracellular matrix degradation and beyond. *Matrix Biology*, 75–76, 141–159. <https://doi.org/10.1016/j.matbio.2018.01.024>
- Wang, Y., Wang, X., Shi, J., Zhu, R., Zhang, J., Zhang, Z., ... Mizuno, M. (2016). A

- biomimetic silk fibroin/sodium alginate composite scaffold for soft tissue engineering. *Scientific Reports*, 6(November), 1–13. <https://doi.org/10.1038/srep39477>
- Xing, H., Lee, H., Luo, L., & Kyriakides, T. R. (2019). Extracellular matrix-derived biomaterials in engineering cell function. *Biotechnology Advances*, (July), 107421. <https://doi.org/10.1016/j.biotechadv.2019.107421>
- Ye, P., Yu, B., Deng, J., She, R. F., & Huang, W. L. (2017). Application of silk fibroin/chitosan/nano-hydroxyapatite composite scaffold in the repair of rabbit radial bone defect. *Experimental and Therapeutic Medicine*, 14(6), 5547–5553. <https://doi.org/10.3892/etm.2017.5231>
- Zhang, S., Xing, M., & Li, B. (2018). Biomimetic layer-by-layer self-assembly of nanofilms, nanocoatings, and 3D scaffolds for tissue engineering. *International Journal of Molecular Sciences*, 19(6). <https://doi.org/10.3390/ijms19061641>
- Zhang, Y. J., Li, M. P., Tang, J., & Chen, X. P. (2017). Pharmacokinetic and pharmacodynamic responses to clopidogrel: Evidences and perspectives. *International Journal of Environmental Research and Public Health*, 14(3). <https://doi.org/10.3390/ijerph14030301>

APPENDICES

APPENDIX 1: ETHICAL APPROVAL DOCUMENT



Date: 12/08/2020

To the Graduate School of Applied Sciences,

For the thesis project entitled as “BIOCOMPATIBILITY STUDIES OF LAYER-BY-LAYER POLYELECTROLYTE COMPLEXES FOR BIOMEDICAL APPLICATIONS”, the researchers declare that they have an approval from the Near East University, Scientific Research Ethical Board with Decision at 23.01.2020, Meeting No: 2020/76 for project No: YDU/2020/76-955.

Title: Doç. Dr.

Name & Surname: Terin Adalı

Signature:



Role in the Research Project: Supervisor

Appendix: I a: Decision Report for the Research Project YDU/2020/76-955.





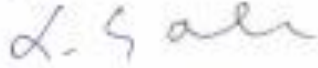
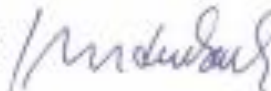


YAKIN DOĞU ÜNİVERSİTESİ
BİLİMSEL ARAŞTIRMALAR ETİK KURULU

EK: 1037-2020

ARAŞTIRMA PROJESİ DEĞERLENDİRME RAPORU

Toplantı Tarihi : 23.01.2020
Toplantı No : 2020/76
Proje No :955

Yakin Dogu Üniversitesi Mühendislik Fakültesi öğretim üyelerinden Doç. Dr. Terin Adalı'nın sorumlu araştırmacısı olduğu, YDU/2020/76-955 proje numaralı ve "Hidrojel Ve Polielektrolit Yapılarda Kan Uyumluluğu Çalışmaları" başlıklı proje önerisi kurulumuzca değerlendirilmiş olup, etik olarak uygun bulunmuştur.

1. Prof. Dr. Rüştü Onur (BAŞKAN) 
2. Prof. Dr. Nerin Bahçeciler Önder (ÜYE) KATILMADI
3. Prof. Dr. Tamer Yılmaz (ÜYE) KATILMADI
4. Prof. Dr. Şahar Saygı (ÜYE) 
5. Prof. Dr. Şanda Çalı (ÜYE) 
6. Prof. Dr. Nedim Çakır (ÜYE) 
7. Prof. Dr. Nurhan Bayraktar (ÜYE) 
8. Doç. Dr. Nilüfer Galip Çelik (ÜYE) KATILMADI
9. Doç. Dr. Emel Mammadov (ÜYE) 
10. Doç. Dr. Mehtap Tınazlı (ÜYE) KATILMADI

APPENDIX II: SIMILARITY REPORT



Submit File		Online Grading Report Edit assignment settings Email non-submitters							
<input type="checkbox"/>	AUTHOR	TITLE	SIMILARITY	GRADE	RESPONSE	FILE	PAPER ID	DATE	
<input type="checkbox"/>	Mthabisi Talent Geor...	Acknowledgment	0%	--	--		1381270546	07-Sep-2020	
<input type="checkbox"/>	Mthabisi Talent Geor...	conclusion	0%	--	--		1381270676	07-Sep-2020	
<input type="checkbox"/>	Mthabisi Talent Geor...	astract	3%	--	--		1381270437	07-Sep-2020	
<input type="checkbox"/>	Mthabisi Talent Geor...	introduction	3%	--	--		1381270797	07-Sep-2020	
<input type="checkbox"/>	Mthabisi Talent Geor...	materials and methods	3%	--	--		1381271747	07-Sep-2020	
<input type="checkbox"/>	Mthabisi Talent Geor...	Literature Review	4%	--	--		1381270940	07-Sep-2020	
<input type="checkbox"/>	Mthabisi Talent Geor...	results	4%	--	--		1381272043	07-Sep-2020	
<input type="checkbox"/>	Mthabisi Talent Geor...	Thesis	8%	--	--		1381272531	07-Sep-2020	

Supervisor: Assoc. Prof. Dr. Terin Adalı

Signature:

A handwritten signature in blue ink, appearing to be "T. Adalı", written over a light blue horizontal line.